NASA TECHNICAL NOTE

NASA TN D-5671

c. 1

NASA TN D-5671

SIMULATION OF THE FOKKER-PLANCK EQUATION BY RANDOM WALKS OF TEST PARTICLES IN VELOCITY SPACE WITH APPLICATION TO MAGNETIC MIRROR SYSTEMS

by Gerald W. Englert

Lewis Research Center
Cleveland, Ohio

NATIONAL AERONAUTICS AND SPACE ADMINISTRATION • WASHINGTON, D. C. • FEBRUARY 1970

1. Report No. NASA TN D-5671	2. Government Accession No.	3. Recipient's Catalog No.
4. Title and Subtitle SIMULATION OF THE FOKKER-PLANCK EQUATION BY RANDOM WALKS OF TEST PARTICLES IN VELOCITY SPACE WITH APPLICATION TO MAGNETIC MIRROR SYSTEMS		5. Report Date February 1970 6. Performing Organization Code
7. Author(s) Gerald W. Englert		8. Performing Organization Report No. E-5165
9. Performing Organization Name and Address Lewis Research Center National Aeronautics and Space Administration Cleveland, Ohio 44135		10. Work Unit No. 120-27 11. Contract or Grant No.
12. Sponsoring Agency Name and Address National Aeronautics and Space Administration Washington, D.C. 20546		13. Type of Report and Period Covered Technical Note 14. Sponsoring Agency Code

15. Supplementary Notes

16. Abstract

The structure of an analytical expression obtained from a random-walk process was compared with that of the Fokker-Planck equation. The step sizes and probabilities of taking steps in various directions were related to the coefficients of the Fokker-Planck equation. Spherical coordinates with azimuthal symmetry about the polar axis were used. The technique was applied to a magnetic-mirror system for confining charged particles. The cases selected have approximate analytical solutions via the Fokker-Planck equation. Velocity distributions inside and end losses from this system were determined by the random-walk procedure and compared with results of the analytical solutions.

17. Key Words (Suggested by Author(s))

Plasma physics
Test particles
Fokker Planck
Random walk
Confinement
Magnetic mirror
Scattering
End loss

18. Distribution Statement

Unclassified - unlimited

19. Security Classif. (of this report)	20. Security Classif. (of this page)	21. No. of Pages	22. Price*
Unclassified	Unclassified	77	$3.00

*For sale by the Clearinghouse for Federal Scientific and Technical Information
Springfield, Virginia 22151

CONTENTS

SIMULATION OF THE FOKKER-PLANCK EQUATION BY RANDOM WALKS OF TEST PARTICLES IN VELOCITY SPACE WITH APPLICATION TO MAGNETIC MIRROR SYSTEMS

by Gerald W. Englert

Lewis Research Center

SUMMARY

The structure of an analytical expression obtained from a random-walk process was compared with that of the Fokker-Planck equation. The step sizes and probabilities of taking steps in various directions were related to the coefficients of the Fokker-Planck equation. Spherical coordinates with azimuthal symmetry about the polar axis were used.

The technique was applied to a magnetic-mirror system for confining charged particles. The cases selected have approximate analytical solution via the Fokker-Planck equation. Velocity distributions inside and end losses from this system were determined by the random-walk procedure and compared with results of the analytical solutions.

The effect of reducing the maximum impact parameter cutoff distance well below the Debye length was studied. This reduction increased step sizes and decreased collision frequency in such a manner that the probability of a test particle walking to specified locations in velocity space remained approximately constant. A sampling of random numbers from the lower impact-parameter range greatly reduced computing time and yet permitted reliable distributions within 10- to 20-percent accuracy.

The random-walk results were, in turn, permitted an appraisal of some simplifying assumptions made in the analytical solution of the Fokker-Planck equation. An iteration procedure was used to find a self-consistent solution of the distribution of test particles walking through an ensemble of field particles, on which the Fokker-Planck coefficients were based. Analytical solutions assume that the distribution of test particles and loss rates are insensitive to assumed field-particle distributions. For the cases studied this was found to be a good assumption. Two steps in the iteration process made the random-walk solutions self-consistent within the scattering of the data for a sampling size of 500 test particles. The popular assumption of separability of the distribution function was also verified.

The random-walk method should apply with little additional difficulty to a number of problems that cannot be solved analytically.

INTRODUCTION

The Fokker-Planck equation, in general, describes the time development of a Markov process. Such a process is characteristic of the nature of classical collisions where each event depends on the present conditions and is independent of the past (ref. 1, p. 157, and ref. 2, p. 369). Written in velocity space, this equation provides a popular approximation to the collisional terms in the Boltzmann equation (refs. 3 to 5). Included in this approximation are first and second moments of velocity increments describing two-body encounters (p. 75 of ref. 6). These moments enter as coefficients of the Fokker-Planck equation and permit it to describe changes in the velocity distribution function resulting from influence of dynamic friction and dispersion (refs. 7 and 8). In general, the velocity distribution function is used to weight the moments of velocity increments, making the Fokker-Planck equation nonlinear and very difficult to solve for many problems of interest.

Another approach to collision problems is through the study of random walks of test particles. This approach replaces the mathematical complexity with a relatively simple but repetitious process, which is greatly facilitated by high-speed computers. Usually the walks of a large sample of test particles through an ensemble of field particles must be studied to determine how they distribute in velocity space. For a self-consistent solution, the resulting test-particle distribution should coincide with the field-particle distribution, requiring an iteration process.

A random walk will be defined herein as a process in which step sizes and probabilities of taking various steps are average values (depending on field-particle distributions and test-particle location in velocity space for the case at hand). In contrast to this procedure is the more popular Monte Carlo method. This technique makes random selections from distributions of pertinent variables (such as impact parameter and relative velocity) at each collision and performs an interaction calculation at each step to determine the resulting test-particle location (refs. 9 and 10). Such a detailed calculation at each step is excellent for physical and mathematical clarity, but would involve an excessive amount of computer time for cases involving a very large number of encounters. On the other hand some physical clarity can be easily lost in the representation by random walks, especially in determining the probability of taking steps in various directions. The ability to relate step sizes and probabilities to the well explored coefficients of the Fokker-Planck equation would thus be very useful.

The random-walk and the Fokker-Planck concepts depend primarily on the same combinatory laws of probability; however, the random walk as depicted herein is restricted to steps on a grid. A detailed generation of the Fokker-Planck equation from a random-walk procedure is available in the literature only for the one-dimensional problem with constant coefficients. Reference 2 (ch. 14) shows that for this case the proper step size of a random walk is dependent on the second moment and that the probabilities

of taking steps in positive and negative directions depend on both first and second moments. This derivation is extended herein to problems involving three dimensions and variable coefficients. In this more general case the step sizes and probabilities are again determined in terms of Fokker-Planck coefficients. The Fokker-Planck coefficients are evaluated for the binary Coulomb encounters used in plasma physics.

A main difficulty in obtaining final results is due to the long range nature of Coulomb encounters, which makes the step sizes of the walks extremely small. For example, at typical experimental or laboratory conditions, a particle may average 10^7 encounters (steps) before it reaches a 90° deflection from its initial direction. At thermonuclear conditions this number easily reaches 10^{16} steps. Tracing such a large number of steps for a representative number of test particles would require an excessive amount of time even for today's fastest computers. A selective sampling technique of some nature must be therefore employed to the random-walk procedure.

The coefficients of the Fokker-Planck equation are insensitive to the cutoff assumed for the collisional impact parameter (refs. 11 and 12). As the maximum impact parameter is reduced, the average step size increases, but the number of encounters (steps) per unit time decreases. With a low impact-parameter cutoff distance a test particle would take a relatively small number of large steps. On the average, however, it would reach a specified boundary in velocity space in about the same time as in a walk based on a higher impact-parameter cutoff and requiring a large number of small steps. The computing time, however, varies inversely as about the square of the step size and is thus much less for walks based on lower impact-parameter cutoff distances.

To study results of this sampling technique, it was applied to the end-loss problem of magnetic-mirror systems. The scattering of charged particles into a loss cone has received considerable attention over a period of years. However, because of the complexity of the Fokker-Planck equation, the rate of such loss has been determined analytically for only the simplest of cases (refs. 5 and 3). Numerical solutions (ref. 13) are available for only a restrictive set of initial and boundary conditions. Desired also are particle distributions inside the mirror system for use in stability studies (ref. 14).

In summarizing, the attempt herein is to exchange a difficult analytical problem with a fairly straightforward computing procedure. Computing time is made reasonable by a sampling technique. Considerable physical detail can be incorporated into such a procedure with little increase of mathematical complexity.

ANALYSIS

The general form of a random-walk equation will be derived for walking on a coordinate grid in N dimensions. (One-dimensional walks with constant step sizes and probabilities are treated in refs. 2 and 8. Ref. 2 writes the results in the form of a

Fokker-Planck differential equation. Ref. 8 uses the random walk to derive solutions to some boundary value problems, but does not arrive at a differential equation as an intermediate step. The Fokker-Planck equation is also derived in ref. 8, but not from the concept of a random walk on a grid.) It is not necessary for the grid to be orthogornal or have constant spacing. Comparison will then be made with the Fokker-Planck equation applied to inverse square collisions in velocity space. The results will be adapted to a study of charged particles in a magnetic-mirror system.

A list of symbols is given in appendix A. The International System of Units (SI) will be used throughout with the exception of temperature T being reported in keV and the corresponding Boltzmann constant k in joules per keV.

Development of the Random-Walk Equation

Let $\xi_1, \xi_2, \ldots, \xi_N$ be independent coordinates that span the space of interest. Let p_i and q_i be the probabilities that the i^{th} coordinate will increase or decrease during the course of a step. To identify these conditional probabilities, only their location at the start of a step will be labeled in their arguments. For example, compared with the more conventional nomenclature,

$$p_1(\xi_1, \xi_2, \ldots, \xi_N)$$

means

$$p_1(\xi_1 + \Delta\xi_1, \xi_2, \ldots, \xi_N | \xi_1, \xi_2, \ldots, \xi_N)$$

and

$$q_1(\xi_1, \xi_2, \ldots, \xi_N)$$

means

$$q_1(\xi_1 - \Delta\xi_1, \xi_2, \ldots, \xi_N | \xi_1, \xi_2, \ldots, \xi_N)$$

Let the probability of a step being in the $\pm i^{th}$ direction be $1/N$; that is,

$$p_i(\xi_1, \xi_2, \ldots, \xi_N) + q_i(\xi_1, \xi_2, \ldots, \xi_N) = \frac{1}{N} \tag{1}$$

Let $u_n(\xi_1, \xi_2, \ldots, \xi_N)$ denote the chance of a particle being at location

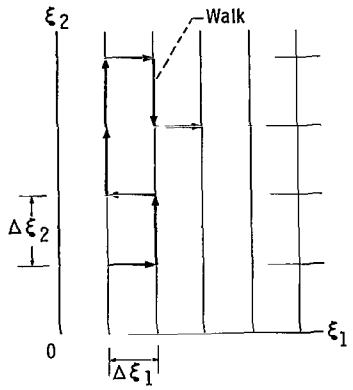

(a) Steps along component directions; number of components changed per encounter, 1.

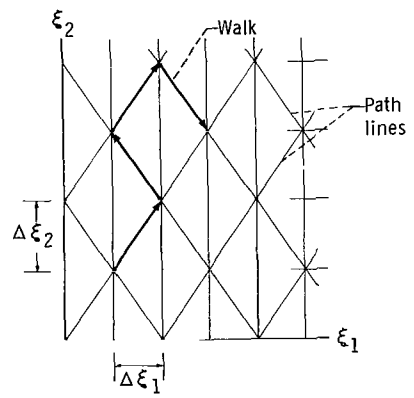

(b) Steps along diagonals; number of components changed per encounter, 2.

Figure 1. - Examples of random walks in two-dimensional Cartesian coordinates.

$(\xi_1, \xi_2, \ldots, \xi_N)$ at the start of the n^{th} step and Δt be the time interval between starts of the n and $n + \eta$ steps.

Consider the case for $\eta = 1$, illustrated in figure 1(a). The change in the number of particles at $(\xi_1, \xi_2, \ldots, \xi_N)$ during Δt is the probability of reaching $(\xi_1, \xi_2, \ldots, \xi_N)$ from the closest neighbors minus the chance of a particle leaving $(\xi_1, \xi_2, \ldots, \xi_N)$ and going to a nearest neighbor. Since a step of finite size is taken each time increment, there is no chance of a particle standing still. The conservation of particles at $(\xi_1, \xi_2, \ldots, \xi_N)$ can thus be written

$$u_{n+1}(\xi_1, \xi_2, \ldots, \xi_N) - u_n(\xi_1, \xi_2, \ldots, \xi_N) = p_1(\xi_1 - \Delta\xi_1, \xi_2, \ldots, \xi_N)u_n(\xi_1 - \Delta\xi_1, \xi_2, \ldots, \xi_N)$$

$$+ q_1(\xi_1 + \Delta\xi_1, \xi_2, \ldots, \xi_N)u_n(\xi_1 + \Delta\xi_1, \xi_2, \ldots, \xi_N)$$

$$+ p_2(\xi_1, \xi_2 - \Delta\xi_2, \ldots, \xi_N)u_n(\xi_1, \xi_2 - \Delta\xi_2, \ldots, \xi_N)$$

$$+ q_2(\xi_1, \xi_2 + \Delta\xi_2, \ldots, \xi_N)u_n(\xi_1, \xi_2 + \Delta\xi_2, \ldots, \xi_N)$$

$$+ \ldots + p_N(\xi_1, \xi_2, \ldots, \xi_N - \Delta\xi_N)u_n(\xi_1, \xi_2, \ldots, \xi_N - \Delta\xi_N)$$

$$+ q_N(\xi_1, \xi_2, \ldots, \xi_N + \Delta\xi_N)u_n(\xi_1, \xi_2, \ldots, \xi_N + \Delta\xi_N)$$

$$- p_1(\xi_1, \xi_2, \ldots, \xi_N)u_n(\xi_1, \xi_2, \ldots, \xi_N) - q_1(\xi_1, \xi_2, \ldots, \xi_N)u_n(\xi_1, \xi_2, \ldots, \xi_N)$$

$$- p_2(\xi_1, \xi_2, \ldots, \xi_N)u_n(\xi_1, \xi_2, \ldots, \xi_N) - q_2(\xi_1, \xi_2, \ldots, \xi_N)u_n(\xi_1, \xi_2, \ldots, \xi_N)$$

$$- \ldots - p_N(\xi_1, \xi_2, \ldots, \xi_N)u_n(\xi_1, \xi_2, \ldots, \xi_N) - q_N(\xi_1, \xi_2, \ldots, \xi_N)u_n(\xi_1, \xi_2, \ldots, \xi_N)$$

where use is made of the first and second laws of composition of probability.

Multiplying through by 2N and adding and subtracting u_n *terms results in*

$$2N[u_{n+1}(\xi_1, \xi_2, \ldots, \xi_N) - u_n(\xi_1, \xi_2, \ldots, \xi_N)] = Np_1(\xi_1 - \Delta\xi_1, \xi_2, \ldots, \xi_N)u_n(\xi_1 - \Delta\xi_1, \xi_2, \ldots, \xi_N)$$

$$- [1 - Np_1(\xi_1 - \Delta\xi_1, \xi_2, \ldots, \xi_N)u_n(\xi_1 - \Delta\xi_1, \xi_2, \ldots, \xi_N)$$

$$+ Nq_1(\xi_1 + \Delta\xi_1, \xi_2, \ldots, \xi_N)u_n(\xi_1 + \Delta\xi_1, \xi_2, \ldots, \xi_N)$$

$$- [1 - Nq_1(\xi_1 + \Delta\xi_1, \xi_2, \ldots, \xi_N)]u_n(\xi_1 + \Delta\xi_1, \xi_2, \ldots, \xi_N)$$

$$+ u_n(\xi_1 - \Delta\xi_1, \xi_2, \ldots, \xi_N) - 2u_n(\xi_1, \xi_2, \ldots, \xi_N) + u_n(\xi_1 + \Delta\xi_1, \xi_2, \ldots, \xi_N)$$

$$+ Np_2(\xi_1, \xi_2 - \Delta\xi_2, \ldots, \xi_N)u_n(\xi_1, \xi_2 - \Delta\xi_2, \ldots, \xi_N)$$

$$- [1 - Np_2(\xi_1, \xi_2 - \Delta\xi_2, \ldots, \xi_N)]u_n(\xi_1, \xi_2 - \Delta\xi_2, \ldots, \xi_N)$$

$$+ Nq_2(\xi_1, \xi_2 + \Delta\xi_2, \ldots, \xi_N)u_n(\xi_1, \xi_2, \ldots, \xi_N)$$

$$- [1 - Nq_2(\xi_1, \xi_2 + \Delta\xi_2, \ldots, \xi_N)]u_n(\xi_1, \xi_2 + \Delta\xi_2, \ldots, \xi_N)$$

$$+ u_n(\xi_1, \xi_2 - \Delta\xi_2, \ldots, \xi_N) - 2u_n(\xi_1, \xi_2, \ldots, \xi_N) + u_n(\xi_1, \xi_2 + \Delta\xi_2, \ldots, \xi_N)$$

$$+ \ldots + Np_N(\xi_1, \xi_2, \ldots, \xi_N - \Delta\xi_N)u_n(\xi_1, \xi_2, \ldots, \xi_N - \Delta\xi_N)$$

$$- [1 - Np_N(\xi_1, \xi_2, \ldots, \xi_N - \Delta\xi_N)]u_n(\xi_1, \xi_2, \ldots, \xi_N - \Delta\xi_N)$$

$$+ Nq_N(\xi_1, \xi_2, \ldots, \xi_N + \Delta\xi_N)u_n(\xi_1, \xi_2, \ldots, \xi_N + \Delta\xi_N)$$

$$- [1 - Nq_N(\xi_1, \xi_2, \ldots, \xi_N + \Delta\xi_N)]u_n(\xi_1, \xi_2, \ldots, \xi_N + \Delta\xi_N)$$

$$+ u_n(\xi_1, \xi_2, \ldots, \xi_N - \Delta\xi_N) - 2u_n(\xi_1, \xi_2, \ldots, \xi_N) + u_n(\xi_1, \xi_2, \ldots, \xi_N + \Delta\xi_N)$$

Using equation (1), combining p_i and q_i terms of like arguments and i subscripts, collecting u_n terms and finally writing the result in finite difference notation yields

$$2\frac{\Delta u}{\Delta n}\Delta n = 2\frac{\Delta u}{\Delta t}\Delta t = -2\left\{\delta_1[(p_1 - q_1)u_n] + \delta_2[(p_2 - q_2)u_2] + \ldots + \delta_N[(p_N - q_N)u_n]\right\} + \frac{1}{N}(\delta_{11}u_n + \delta_{22}u_n + \ldots + \delta_{NN}u_n)$$

which approaches the limit

$$\frac{\partial u}{\partial t} = \sum_{i=1}^{N}\left\{-\frac{\partial\left[(p_i - q_i)u\right]}{\partial \xi_i}\frac{\Delta \xi_i}{\Delta t} + \frac{1}{2}\frac{\partial^2 u}{\partial \xi_i^2}\frac{(\Delta \xi_i)^2}{N\,\Delta t}\right\}$$

as step size (grid spacing) becomes arbitrarily small.

This is the more conventional approach to a random-walk expression. However, next consider the case where steps are taken in groups of $\eta = N$; one along each coordinate direction. (This corresponds to the later physical description of a test particle in polar coordinates where its magnitude and direction (v, θ, and φ) change each encounter.) This corresponds to steps across the diagonals of N-dimensional lattices which will herein be called path lines. This is illustrated for the case of $N = 2$ on figure 1(b).

Repeating this procedure with $\eta = N$ gives

$$\frac{\partial u}{\partial t} = \sum_{i=1}^{N}\left\{-\frac{\partial\left[N(p_i - q_i)u\right]}{\partial \xi_i}\frac{\Delta \xi_i}{\Delta t} + \frac{1}{2}\frac{\partial^2 u}{\partial \xi_i^2}\frac{(\Delta \xi_i)^2}{\Delta t}\right\} \tag{2}$$

This same result could be obtained by letting

$$p_i(\xi_1, \xi_2, \ldots, \xi_N) + q_i(\xi_1, \xi_2, \ldots, \xi_N) = 1 \qquad i = 1, 2, \ldots, N$$

in the derivation regardless of N, and letting $\eta = 1$; that is, there is a sure chance of stepping either in the plus or minus direction of each of the components for each time increment Δt.

Equation (2) is in the form of the Fokker-Planck equation except that no mixed

partial derivatives are present. Generation of these terms does not appear possible when the walks are restricted to the nearest neighbors on a grid. Their magnitude will be discussed later.

Note that $p_i - q_i$ is like a bias in the i^{th} direction and that the terms involving first-order derivatives could be, for example, related to friction. To keep the process from being degenerate, $p_i - q_i$ must approach zero as step size approaches zero (p. 324 of ref. 2). The terms involving second derivatives are similar to diffusion expressions with $(\Delta\xi_i)^2/\Delta t$ similar to a diffusion coefficient.

When a stochastic process is being simulated by a random walk on a grid, the step sizes are often statistical averages. It can be deduced from references 2, 8, 15, or 16 that second moments determine the proper grid spacing. Consider, for example, the application discussed in the next section. In any small region of velocity space the test particle taking a random walk encounters many other field or background particles, one at a time. A field particle can be in any accessible region of velocity space as it starts its encounter with a test particle (its probable location is defined by appropriate distribution functions). The grid spacings are thus based on statistical averages of encounters with field particles (fig. 2), these averages nevertheless being dependent on test-particle location.

p_i and q_i Probabilities of increase and decrease, respectively, of i^{th} component ($i = 1, 2, 3$)

$\sqrt{\overline{(\Delta v_i)^2}}$ i^{th} component of step size

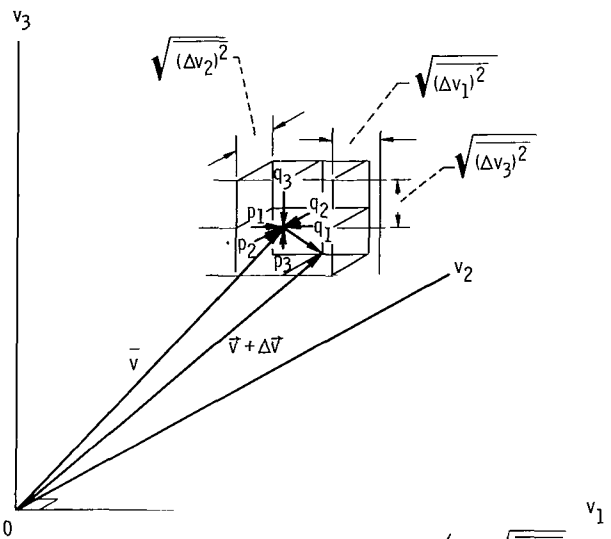

Figure 2. - Example of step from (v_1, v_2, v_3) to $\left(v_1 + \sqrt{\overline{(\Delta v_1)^2}}, v_2 + \sqrt{\overline{(\Delta v_2)^2}}, v_3 - \sqrt{\overline{(\Delta v_3)^2}}\right)$.

Fokker-Planck Equation

The widely accepted Fokker-Planck equation for studying plasmas in N dimensional Cartesian coordinates is

$$\left(\frac{\partial f}{\partial t}\right)_c = \sum_{i,j=1}^{N} -\frac{\partial}{\partial v_i}\left(f\langle \Delta v_i\rangle\right) + \frac{1}{2}\frac{\partial^2}{\partial v_i\, \partial v_j}\left(f\langle \Delta v_i\, \Delta v_j\rangle\right)$$

where $(\partial f/\partial t)_c$ denotes the change of probability density (distribution function of test particles) with respect to time due to collisions. The coefficients $\langle \Delta v_i\rangle$ and $\langle \Delta v_i\, \Delta v_j\rangle$ are averages over distributions of field particles and scattering angle (ref. 11). The angular brackets signify a time average; that is, $\langle \Delta v_i\rangle$ is the average increment per unit time of the i^{th} component of velocity. The average value per collision, denoted by a bar, is equal to the time average divided by the collision frequency ν; for example, $\overline{\Delta v_i} = \langle \Delta v_i\rangle/\nu$.

The Fokker-Planck equation is transformed to spherical coordinates with symmetry about the polar axis in appendix B. This is essentially the same coordinate system as used in parts IV and V of reference 11. In reference 11, $\cos\theta$ is used in place of the polar angle θ used herein. The assumption of aximuthal symmetry is not too restrictive for many problems in plasma physics and serves mainly to reduce cumbersome expressions. The analysis follows in a straightforward manner without it. In this coordinate system

$$\left(\frac{\partial f}{\partial t}\right)_c = -\frac{1}{v^2}\frac{\partial}{\partial v}\left(v^2 f\langle \Delta v\rangle\right) - \frac{1}{\sin\theta}\frac{\partial}{\partial \theta}\left(f \sin\theta \langle \Delta\theta\rangle\right) + \frac{1}{2v^2}\frac{\partial^2 v^2 f\langle (\Delta v)^2\rangle}{\partial v^2} + \frac{1}{2\sin\theta}\frac{\partial^2 f \sin\theta \langle (\Delta\theta)^2\rangle}{\partial\theta^2}$$

$$+ \frac{1}{v^2 \sin\theta}\frac{\partial^2 v^2 f \sin\theta \langle \Delta v\, \Delta\theta\rangle}{\partial v\, \partial\theta} - \frac{1}{2v^2}\frac{\partial}{\partial v}\left\{v^3 f\left[\langle (\Delta\theta)^2\rangle + \sin^2\theta \langle (\Delta\varphi)^2\rangle\right]\right\}$$

$$+ \frac{1}{2v \sin\theta}\frac{\partial}{\partial\theta}\left\{f \sin\theta\left[2\langle \Delta\theta\, \Delta v\rangle - v \sin\theta \cos\theta \langle (\Delta\varphi)^2\rangle\right]\right\}$$

Using the identities

$$\frac{\partial^2 v^2 f\langle(\Delta v)^2\rangle}{\partial v^2} = \langle(\Delta v)^2\rangle \frac{\partial^2 v^2 f}{\partial v^2} + 2\frac{\partial}{\partial v}\left(v^2 f \frac{\partial\langle(\Delta v)^2\rangle}{\partial v}\right) - v^2 f \frac{\partial^2\langle(\Delta v)^2\rangle}{\partial v^2}$$

and

$$\frac{\partial^2 f \sin\theta\langle(\Delta\theta)^2\rangle}{\partial\theta^2} = \langle(\Delta\theta)^2\rangle \frac{\partial^2 f \sin\theta}{\partial\theta^2} + 2\frac{\partial}{\partial\theta}\left(f \sin\theta \frac{\partial\langle(\Delta\theta)^2\rangle}{\partial\theta}\right) - f \sin\theta \frac{\partial^2\langle(\Delta\theta)^2\rangle}{\partial\theta^2}$$

the Fokker-Planck equation can be written as

$$\left(\frac{\partial f}{\partial t}\right)_c + \frac{f}{2}\left(\frac{\partial^2\langle(\Delta v)^2\rangle}{\partial v^2} + \frac{\partial^2\langle(\Delta\theta)^2\rangle}{\partial\theta^2}\right) = -\frac{1}{v^2}\frac{\partial}{\partial v}\left[v^2 f\langle\Delta v\rangle - \frac{\partial\langle(\Delta v)^2\rangle}{\partial v} + \frac{v}{2}\langle(\Delta\theta)^2\rangle + \frac{v}{2}\sin^2\theta\langle(\Delta\varphi)^2\rangle\right]$$

$$-\frac{1}{\sin\theta}\frac{\partial}{\partial\theta}\left[f \sin\theta\left(\langle\Delta\theta\rangle - \frac{\partial\langle(\Delta\theta)^2\rangle}{\partial\theta} - \frac{\langle\Delta\theta\,\Delta v\rangle}{v} + \frac{\sin\theta\cos\theta}{2}\langle(\Delta\varphi)^2\rangle\right)\right] + \frac{1}{v^2 \sin\theta}\frac{\partial^2 v^2 f \sin\theta\langle\Delta v\,\Delta\theta\rangle}{\partial v\,\partial\theta}$$

$$+\frac{\langle(\Delta v)^2\rangle}{2v^2}\frac{\partial^2 f v^2}{\partial v^2} + \frac{\langle(\Delta\theta)^2\rangle}{2\sin\theta}\frac{\partial^2 f \sin\theta}{\partial\theta^2} \tag{3}$$

Correspondence Between the Random-Walk and Fokker-Planck Equations

The random-walk expression (eq. (2)) describes the average results of a large number of walks, or a large number of walks gives a numerical solution to the random-walk equation. An attempt will now be made to write equation (2) in a form in close agreement with equation (3) to see whether random walks can provide solutions to the Fokker-Planck equation.

In equation (2) let $N = 2$, $\xi_1 = v$, $\xi_2 = \theta$, and $\Delta t = 1/\nu$ (where $\nu = \nu(v, \theta)$ = collision frequency). By equation (1) $p_1 + q_1 = 1/2$ and $p_2 + q_2 = 1/2$. Let

$$2(p_1 - q_1) = \frac{\left[\overline{\Delta v} - \frac{1}{\nu}\frac{\partial\langle(\Delta v)^2\rangle}{\partial v} + \frac{v}{2}\overline{(\Delta\theta)^2} + \frac{v\sin^2\theta}{2}\overline{(\Delta\varphi)^2}\right]}{\sqrt{\overline{(\Delta v)^2}}}$$

$$2(p_2 - q_2) = \frac{\left[\overline{\Delta\theta} - \frac{1}{\nu}\frac{\partial\langle(\Delta\theta)^2\rangle}{\partial\theta} - \frac{\overline{\Delta\theta\,\Delta v}}{v} + \frac{\sin\theta\cos\theta}{2}\overline{(\Delta\varphi)^2}\right]}{\sqrt{\overline{(\Delta\theta)^2}}} \qquad (4)$$

$$\Delta\xi_1 = \sqrt{\overline{(\Delta v)^2}}$$

$$\Delta\xi_2 = \sqrt{\overline{(\Delta\theta)^2}}$$

and

$$u = fv^2\sin\theta$$

The random-walk equation then becomes

$$\left(\frac{\partial f}{\partial t}\right)_c - \frac{f}{2}\left[\left(\langle\Delta v\rangle - \frac{\partial\langle(\Delta v)^2\rangle}{\partial v} + \frac{v}{2}\langle(\Delta\theta)^2\rangle + \frac{v\sin^2\theta}{2}\langle(\Delta\varphi)^2\rangle\right)\left(\frac{1}{\langle(\Delta v)^2\rangle}\frac{\partial\langle(\Delta v)^2\rangle}{\partial v} + \frac{1}{\nu}\frac{\partial\nu}{\partial v}\right)\right.$$

$$\left. + \left(\langle\Delta\theta\rangle - \frac{\partial\langle(\Delta\theta)^2\rangle}{\partial\theta} - \frac{\langle\Delta\theta\,\Delta v\rangle}{v} + \frac{\sin\theta\cos\theta}{2}\langle(\Delta\varphi)^2\rangle\right)\left(\frac{1}{\langle(\Delta\theta)^2\rangle}\frac{\partial\langle(\Delta\theta)^2\rangle}{\partial\theta} + \frac{1}{\nu}\frac{\partial\nu}{\partial\theta}\right)\right]$$

$$= -\frac{1}{v^2}\frac{\partial}{\partial v}\left[v^2 f\left(\langle\Delta v\rangle - \frac{\partial\langle(\Delta v)^2\rangle}{\partial v} + \frac{v}{2}\langle(\Delta\theta)^2\rangle + \frac{v\sin^2\theta}{2}\langle(\Delta\varphi)^2\rangle\right)\right] \qquad (5)$$

$$-\frac{1}{\sin\theta}\frac{\partial}{\partial\theta}\left[f\sin\theta\left(\langle\Delta\theta\rangle - \frac{\partial\langle(\Delta\theta)^2\rangle}{\partial\theta} - \frac{\langle\Delta\theta\,\Delta v\rangle}{v} + \frac{\sin\theta\cos\theta}{2}\langle(\Delta\varphi)^2\rangle\right)\right] + \frac{1}{2}\frac{\langle(\Delta v)^2\rangle}{v^2}\frac{\partial^2 v^2 f}{\partial v^2} + \frac{1}{2}\frac{\langle(\Delta\theta)^2\rangle}{\sin\theta}\frac{\partial^2 f\sin\theta}{\partial\theta^2}$$

which differs from the Fokker-Planck equation by the terms involved with $f/2$ on the left side of the equal sign, and by the absence of the mixed derivative term on the right side.

To study these equations further and to perform random walks, one must specify the initial and/or boundary conditions. To evaluate the Fokker-Planck coefficients, one must specify the type of encounter. The differences between equations (3) and (5) will be appraised for specific conditions.

Physical Application

The preceding results will be applied to magnetic mirror systems used to confine ensembles of electrically charged particles. The Fokker-Planck coefficients will thus be based on Coulomb encounters. The random walks will determine the ion distributions inside and the end loss from a magnetic mirror system. Such a system is sketched in figure 3 and discussed, along with simplifying assumptions, in appendix C. The velocity space of prime interest can be best described in spherical coordinates (fig. 4). The polar axis is alined with the magnetic field about which there is axial symmetry. This $\vec{B}$ field is assumed to be uniform over the central portion of the physical space. The increased magnitude of $\vec{B}$ at the mirrors enters the problem by describing a loss-cone boundary condition in velocity space. The random walks terminate at this boundary as if it were an absorbing wall. These assumptions result in uniformity of f in φ and in coordinate space and, thus, reduce a problem in six-dimensional phase space to two dimensions in velocity space.

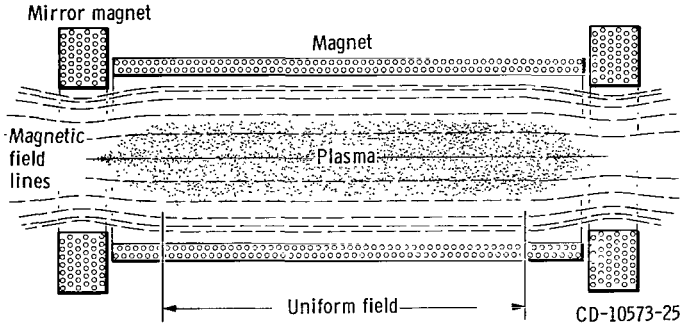

Figure 3. - Magnetic mirror system.

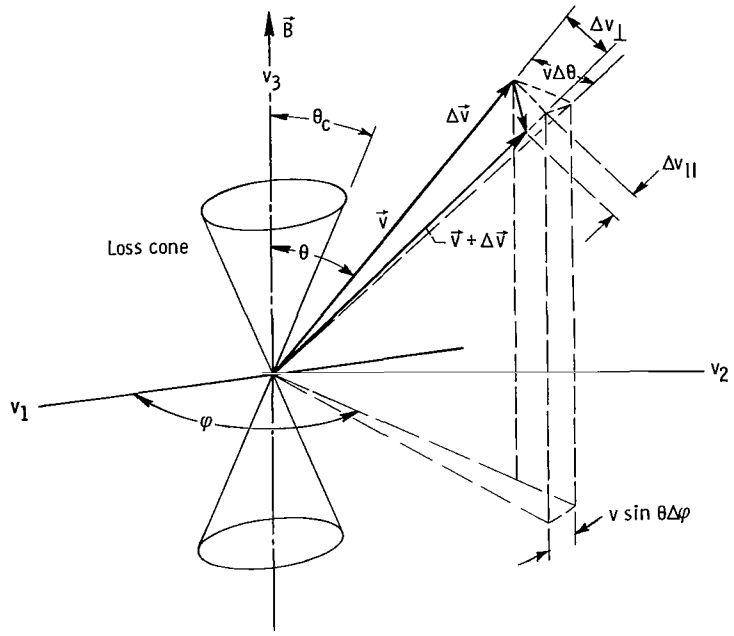

Figure 4. - Spherical coordinates.

The usual simplifying assumptions applied to the analysis of magnetic mirror systems reduce the Boltzmann equation to

$$\left(\frac{\partial f}{\partial t}\right)_c = -\dot{s} \tag{6}$$

for steady state (appendix C). The symbol $\dot{s}$ represents a sink (or source) density in velocity space. For a steady state the rate of particles being injected into the system equals the rate of particles entering the loss cone. Loss rates from the system can therefore be expressed as

$$\dot{n} = -\int \dot{s}(\vec{v})d\vec{v} \tag{7}$$

where integration is over the velocity space of the injection distribution. The injection distribution provides the initial condition for the random walk.

To correct the random-walk results for the difference in the expressions on the left sides of equations (3) and (5), the following equation can be used:

$$\dot{n}_{corrected} = \dot{n}_{random\ walk} - \int \frac{f}{2}\left\{\frac{\partial^2\langle(\Delta v)^2\rangle}{\partial v^2} + \frac{\partial^2\langle(\Delta\theta)^2\rangle}{\partial\theta^2} + \left[\left(\langle\Delta v\rangle - \frac{\partial\langle(\Delta v)^2\rangle}{\partial v} + \frac{v}{2}\langle(\Delta\theta)^2\rangle + \frac{v\sin^2\theta}{2}\langle(\Delta\varphi)^2\rangle\right)\left(\frac{1}{\langle(\Delta v)^2\rangle}\frac{\partial\langle(\Delta v)^2\rangle}{\partial v} + \frac{1}{\nu}\frac{\partial\nu}{\partial v}\right)\right.\right.$$

$$\left.\left. + \left(\langle\Delta\theta\rangle - \frac{\partial\langle(\Delta\theta)^2\rangle}{\partial\theta} - \frac{\langle\Delta\theta\ \Delta v\rangle}{v} + \frac{\sin\theta\cos\theta}{2}\langle(\Delta\varphi)^2\rangle\right)\left(\frac{1}{\langle(\Delta\theta)^2\rangle}\frac{\partial\langle(\Delta\theta)^2\rangle}{\partial\theta} + \frac{1}{\nu}\frac{\partial\nu}{\partial\theta}\right)\right]\right\}d\vec{v} \tag{8}$$

The magnitude of this integral was negligible for cases of most interest. (This will be discussed later.) When the mixed-derivative term of the Fokker-Planck equation is negligible, such as for near isotropic field distributions, $\dot{n}_{corrected}$ is equal to that determined from the Fokker-Planck equation.

Fokker-Planck Coefficients

Expressions for the Fokker-Planck coefficients for the preceding physical application will now be supplied so that the step sizes and probabilities of equations (4) can be determined.

The general integral expressions for these coefficients are derived in appendix D and can be expressed as

$$\langle\Delta v\rangle = -2\Gamma\int \frac{v - v_b\cos\vartheta_r}{\left(v^2 + v_b^2 - 2vv_b\cos\vartheta_r\right)^{3/2}} f(\vec{v}_b)d\vec{v}_b \tag{9a}$$

$$\langle\Delta\theta\rangle = -\frac{2\Gamma}{v^2}\int \frac{vv_b\left[\sin\theta\cos\theta_b - \cos\theta\sin\theta_b\cos(\varphi - \varphi_b)\right]}{\left(v^2 + v_b^2 - 2vv_b\cos\vartheta_r\right)^{3/2}} f(\vec{v}_b)d\vec{v}_b \tag{9b}$$

$$\langle\Delta\theta\ \Delta v\rangle = \frac{\Gamma}{v^2}\int \frac{vv_b(v - v_b\cos\vartheta_r)\left[\sin\theta\cos\theta_b - \cos\theta\sin\theta_b\cos(\varphi - \varphi_b)\right]}{\left(v^2 + v_b^2 - 2vv_b\cos\vartheta_r\right)^{3/2}} f(\vec{v}_b)d\vec{v}_b \tag{9c}$$

$$\langle(\Delta v)^2\rangle = \Gamma \int \frac{1}{\left(v^2 + v_b^2 - 2vv_b \cos \vartheta_r\right)^{1/2}} - \frac{(v - v_b \cos \vartheta_r)^2}{\left(v^2 + v_b^2 - 2vv_b \cos \vartheta_r\right)^{3/2}} f(\vec{v}_b) d\vec{v}_b \tag{9d}$$

$$\langle(\Delta\theta)^2\rangle = \frac{\Gamma}{v^4} \int \left\{ \frac{v^2}{\left(v^2 + v_b^2 - 2vv_b \cos \vartheta_r\right)^{1/2}} - \frac{v^2 v_b^2 \left[\sin\theta \cos\theta_b - \cos\theta \sin\theta_b \cos(\varphi - \varphi_b)\right]^2}{\left(v^2 + v_b^2 - 2vv_b \cos \vartheta_r\right)^{3/2}} \right\} f(\vec{v}_b) d\vec{v}_b \tag{9e}$$

$$\langle(\Delta\varphi)^2\rangle = \frac{\Gamma}{v^4 \sin^2\theta} \int \frac{v^2 - \dfrac{vv_b \sin\theta_b \cos(\varphi - \varphi_b)}{\sin\theta}}{\left(v^2 + v_b^2 - 2vv_b \cos \vartheta_r\right)^{1/2}} f(\vec{v}_b) d\vec{v}_b \tag{9f}$$

$$\nu = \frac{4\Gamma\beta^2}{9 \ln \beta} \left(\frac{m}{2kT_b}\right)^2 \int \left(v^2 + v_b^2 - 2vv_b \cos \vartheta_r\right)^{1/2} f(\vec{v}_b) d\vec{v}_b \tag{9g}$$

where β is the ratio of maximum to minimum impact parameter and

$$\Gamma = \frac{(Ze)^4 \ln \beta}{4\pi\epsilon_0^2 m^2} = \frac{0.24\ Z^4 \ln \beta}{A^2}$$

is the interaction parameter.

In the usual problems of interest the field distribution $f(\vec{v}_b)$ is not known. Also, a test particle is usually just a background particle with a special label. Tracing the paths of a large enough sample should determine test-particle distributions, which for a self-consistent solution should be the same as the field-particle distribution. Such a solution can be approached by an iteration procedure. A background distribution is first assumed; the coefficients are calculated; and the paths of a representative number of test particles are traced to determine their distribution. The distribution of test particles in the l^{th} step of this iteration are used for the field-particle distribution in the $l + 1$ step. This process is continued until the field- and test-particle distributions agree within the desired accuracy. The accuracy, or amount of scatter of the final data, in the example worked herein, was mainly set by the number of test particles used.

In the first step of the iteration process, use of a Maxwellian distribution is con-

sistent with the theory of references 5 and 17. It is argued in these references that loss rates should be insensitive to the assumed field-particle distributions. For purposes herein, this may be considered a first-order solution. The insensitivity to field distribution may indicate convergence of the iteration process in a small number of steps.

Maxwellian distribution of field particles. - A Maxwellian field distribution should provide an especially good first approximation to plasmas which are in near equilibrium conditions. An example of such could be inside mirror systems having very high mirror ratios so that field defects due to loss cones would be small.

Since a Maxwellian distribution is isotropic, all first moments of θ are zero. (An isotropic distribution corresponds to the diffusion approximation of ref. 5 and to the use of effective Rosenbluth potentials in ref. 11.) Thus $\langle \Delta\theta\ \Delta v \rangle$ is zero, and the mixed derivative term is absent from equation (3). Use of

$$f(\vec{v}_b)d\vec{v}_b = n_b\left(\frac{m}{2\pi kT_b}\right)^{3/2} v_b^2\, e^{-mv_b^2/2kT_b}\ \sin\theta_b\, d\theta_b\, d\varphi_b\, dv_b \tag{10}$$

and integrating between the limits

$$0 \le v_b \le \infty$$

$$0 \le \theta_b \le \pi$$

$$0 \le \varphi_b \le 2\pi$$

reduces the expressions for the Fokker-Planck coefficients to the following (see appendix D):

$$\langle \Delta v \rangle = \frac{2n_b\Gamma}{v^2}\left[2\sqrt{\frac{m}{2\pi kT_b}}\, v\, e^{-mv^2/2kT_b} - \operatorname{erf}\left(\sqrt{\frac{m}{2\pi T_b}}\, v\right)\right] \tag{11a}$$

$$\langle (\Delta v)^2 \rangle = -\frac{kT_b}{mv}\langle \Delta v \rangle \tag{11b}$$

$$\langle (\Delta\theta)^2 \rangle = \frac{n_b\Gamma}{v^3}\left[\sqrt{\frac{2kT_b}{\pi m}}\,\frac{1}{v}\, e^{-mv^2/2kT_b} + \left(1 - \frac{kT_b}{mv^2}\right)\operatorname{erf}\left(\sqrt{\frac{m}{2kT_b}}\, v\right)\right] \tag{11c}$$

$$\langle(\Delta\varphi)^2\rangle = \frac{1}{\sin^2\theta}\langle(\Delta\theta)^2\rangle \tag{11d}$$

$$\nu = \frac{4n_b(\beta^2 - 1)}{9 \ln \beta}\left(\frac{m}{2kT_b}\right)^2 v\Gamma\left[\sqrt{\frac{2kT_b}{\pi m}}\frac{1}{v}e^{-mv^2/2kT_b} + \left(1 + \frac{kT_b}{mv^2}\right)\operatorname{erf}\left(\sqrt{\frac{m}{2kT_b}}v\right)\right] \tag{11e}$$

Using equations (11) in (3) finally reduces the Fokker-Planck equation to

$$\left(\frac{\partial f}{\partial t}\right)_c + \frac{f}{2}\frac{\partial^2\langle(\Delta v)^2\rangle}{\partial v^2} = -\frac{1}{v^2}\frac{\partial}{\partial v}\left[v^2 f\left(\langle\Delta v\rangle - \frac{\partial\langle(\Delta v)^2\rangle}{\partial v} + v\langle(\Delta\theta)^2\rangle\right)\right] - \frac{\langle(\Delta\theta)^2\rangle}{2\sin\theta}\frac{\partial}{\partial\theta}(f\cos\theta) + \frac{\langle(\Delta v)^2\rangle}{2v^2}\frac{\partial^2 fv^2}{\partial v^2}$$

$$+ \frac{\langle(\Delta\theta)^2\rangle}{2\sin\theta}\frac{\partial^2 f\sin\theta}{\partial\theta^2} \tag{12}$$

An interesting relation among the coefficients of equation (11) is

$$\frac{1}{2v^2}\frac{\partial}{\partial v}\left(v^2\langle(\Delta v)^2\rangle\right) - v\langle(\Delta\theta)^2\rangle = \frac{1}{2}\langle\Delta v\rangle \tag{13}$$

Use of equations (6) and (13) reduces (12) to equation (18.7) of reference 5.

Equation (12) is especially useful because there is an approximate analytical solution to it in reference 5. The random-walk results will later be compared numerically to this solution.

Using equations (11) reduces the random-walk equation (5) to

$$\left(\frac{\partial f}{\partial t}\right)_c - \frac{f}{2}\left[\left(\langle\Delta v\rangle - \frac{\partial\langle(\Delta v)^2\rangle}{\partial v} + v\langle(\Delta\theta)^2\rangle\right)\left(\frac{1}{\langle(\Delta v)^2\rangle}\frac{\partial\langle(\Delta v)^2\rangle}{\partial v} + \frac{1}{\nu}\frac{\partial\nu}{\partial v}\right)\right]$$

$$= -\frac{1}{v^2}\frac{\partial}{\partial v}\left[v^2 f\left(\langle\Delta v\rangle - \frac{\partial\langle(\Delta v)^2\rangle}{\partial v} + v\langle(\Delta\theta)^2\rangle\right)\right] - \frac{\langle(\Delta\theta)^2\rangle}{2\sin\theta}\frac{\partial}{\partial\theta}(f\cos\theta) + \frac{\langle(\Delta v)^2\rangle}{2v^2}\frac{\partial^2 fv^2}{\partial v^2} + \frac{\langle(\Delta\theta)^2\rangle}{2\sin\theta}\frac{\partial^2 f\sin\theta}{\partial\theta^2} \tag{14}$$

In terms of dimensionless variables the average value per collision of the variables in equation (11) can be conveniently written as

$$\Delta V = \frac{\langle \Delta v \rangle}{\nu v_o} = \frac{9}{2} \frac{\ln \beta}{\beta^2} \left(\frac{T_b}{E'_o} \right)^2 \frac{\left[2V \sqrt{\frac{E'_o}{\pi T_b}} e^{-V^2 E'_o / T_b} - \operatorname{erf}\left(V \sqrt{\frac{E'_o}{T_b}} \right) \right]}{V^3 \left[\frac{1}{V} \sqrt{\frac{T_b}{\pi E'_o}} e^{-V^2 E'_o / T_b} + \left(1 + \frac{T_b}{2V^2 E'_o} \right) \operatorname{erf}\left(V \sqrt{\frac{E'_o}{T_b}} \right) \right]} \tag{15a}$$

$$\overline{(\Delta V)^2} = \frac{\langle (\Delta v)^2 \rangle}{2 v_o} = - \frac{T_b}{2 V E'_o} \overline{\Delta V} \tag{15b}$$

$$\overline{(\Delta \theta)^2} = \frac{9}{4} \frac{\ln \beta}{V^4 \beta^2} \left(\frac{T_b}{E'_o} \right)^2 \frac{\left[\frac{1}{V} \sqrt{\frac{T_b}{\pi E'_o}} e^{-V^2 E'_o / T_b} + \left(1 - \frac{T_b}{2V E'_o} \right) \operatorname{erf}\left(V \sqrt{\frac{E'_o}{T_b}} \right) \right]}{\left[\frac{1}{V} \sqrt{\frac{T_b}{\pi E'_o}} e^{-V^2 E'_o / T_b} + \left(1 + \frac{T_b}{2V E'_o} \right) \operatorname{erf}\left(V \sqrt{\frac{E'_o}{T_b}} \right) \right]} \tag{15c}$$

$$\overline{(\Delta \varphi)^2} = \frac{1}{\sin^2 \theta} \overline{(\Delta \theta)^2} \tag{15d}$$

$$\frac{\nu T_b^{3/2} m^{1/2}}{n_b Z^4} = 0.518 \times 10^{-31} \beta^2 V \sqrt{\frac{E'_o}{T_b}} \left[\left(1 + \frac{T_b}{2V^2 E'_o} \right) \operatorname{erf}\left(V \sqrt{\frac{E'_o}{T_b}} \right) + \frac{1}{V \sqrt{\frac{\pi E'_o}{T_b}}} e^{-V^2 E'_o / T_b} \right] \tag{15e}$$

where

$$V = \frac{v}{v_o} \qquad E_o = \frac{1}{2} m v_o^2 \qquad E'_o = \frac{E_o}{k} \qquad \beta >> 1$$

and v_o is some reference test-particle velocity. The quantity E'_o is always referenced to T_b and velocity v is referenced to v_o; thus, v is actually referenced to T_b through E'_o. If $E'_o/T_b = 3/2$, then by the kinetic definition of temperature E_o (p. 37 of ref. 18) is the average field-particle energy, and V is the ratio of the test-particle velocity to the rms field-particle velocity. Thus for most applications herein E'_o/T_b was set equal to 3/2. When studying the case of injection of a monoenergetic beam of test particles into a background ensemble, however, it was convenient to set E_o equal to the beam-particle energy. Thus for example, when the beam particles had an energy of 10 times the average field-particle energy, E_o/T_b was set equal to 15, making the initial value of V equal to 1.

Plots of generalized step sizes $\sqrt{\overline{(\Delta V)^2}}\left(\beta\sqrt{E'_o/T_b}\Big/\sqrt{\ln\beta}\right)$ and $V\sqrt{\overline{(\Delta\theta)^2}}\left(\beta\sqrt{E'_o/T_b}\Big/\sqrt{\ln\beta}\right)$ for a Maxwellian field distribution are shown in figure 5. These curves were obtained by use of equations (15a) to (15c).

Computing time and impact parameter cutoff distance. - Setting the maximum impact parameter at the Debye length and the minimum value at a distance to cause a 90° deflection results in

$$\beta_{\text{Debye}} = \frac{0.49\times10^{18}\,Te_b^{3/2}}{Z^2 n_e^{1/2}} \tag{16}$$

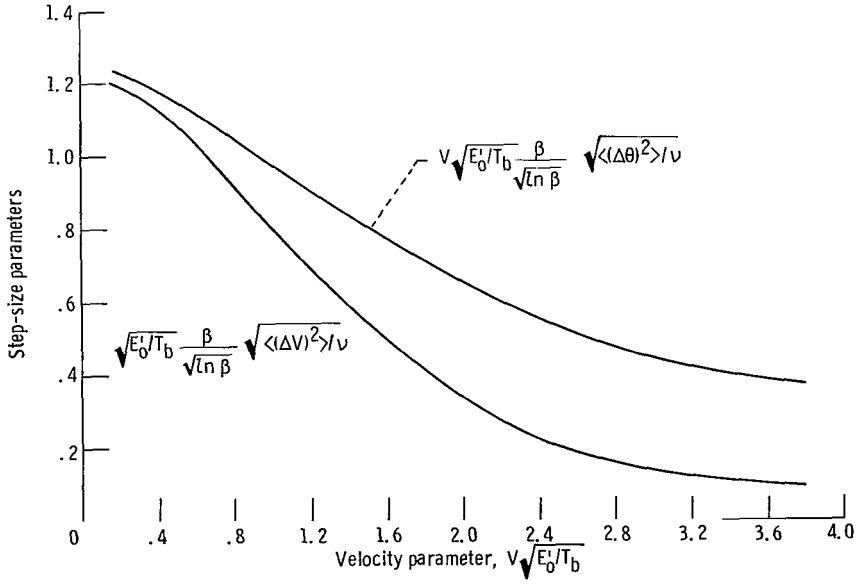

Figure 5. - Generalized step-size parameters in V and θ directions.

for T_b (in Kev) and n_b (in m^{-3}). Numerical values are given in table 5. 1 of reference 12.

If the maximum impact parameter is cutoff at the Debye length as in equation (16), the average deflection which a particle undergoes per collision $\sqrt{(\Delta\theta)^2/\nu}$ is extremely small, as can be deduced from figure 5. Thus the corresponding computing time required to trace representative samples of test particles would be prohibitively large. It was observed from the elementary one-dimensional (and nonbiased) random walks of reference 8 and also from preliminary computer results that the average number of steps to reach a distance m steps away from a starting point was nearly proportional to m^2. The time to take such a walk would thus be nearly proportional to m^2/ν. For a random walk in the θ direction the distance reached per unit time would correspond to $\nu(\Delta\theta)^2$, which is simply the diffusion coefficient $\langle(\Delta\theta)^2\rangle$.

Solutions to processes described by the Fokker-Planck equation are dependent on impact parameter cutoff distance only through the Fokker-Planck coefficients. As shown by equations (9) and (11), these coefficients are only weakly dependent on impact parameter ratio β. It thus appears that a particle taking the fewer number of larger steps determined by a lower β cutoff would reach given locations in velocity space in about the same time as if it took the larger number of smaller steps determined by a higher β cutoff point. The final walk time (loss rate) would possible be weighted by a function of β.

As part of the following computer study, the effect of β on loss rates from and distributions inside magnetic mirror systems was determined. Cases were selected that could be solved analytically for comparison with the random-walk results.

Numerical Procedure

The procedure by which the random walks were simulated by the computer and the manner in which velocity distributions inside and end losses from the magnetic mirror system were obtained from the walks will now be described.

A computer flow diagram and a representative FORTRAN program are presented in appendix E. Either the Lewis IBM 7044-7094 or 7040-7094 direct coupled systems were used to perform the calculations.

Initial conditions for each random walk were determined by selecting at random from prescribed injection distributions. The walks were terminated at the loss-cone boundaries θ_c and $\pi - \theta_c$ where

$$\theta_c = \sin^{-1} \frac{1}{\sqrt{B_c/B_o}} \tag{17}$$

and B_c/B_o is the ratio of the magnetic field at the mirror to that in the central uniform region (ref. 12).

In any of the steady-state models selected for study herein, the average number of particles injected per unit time equals the rate at which particles enter the loss cone. The walks were studied one at a time, and a large enough number of them were traced to form a representative statistical sample.

The velocity space to which the test particles had access was divided into zones. For each of these zones values of probabilities p_1 and p_2, step sizes $\sqrt{\langle(\Delta v)^2\rangle/\nu}$ and $\sqrt{\langle(\Delta\theta)^2\rangle/\nu}$, and collision frequency were computed for the field distribution of interest. These quantities were stored in matrix form and called for as the test particle progressed about the velocity field, as described in appendix E.

During each step of each walk, a random number was selected for each of the two components (V and θ) and compared with probabilities p_1 and p_2, respectively, to determine step direction. These random numbers were selected from a set of numbers uniformly distributed over the interval from 0 to 1 (ref. 10). Whether the V component of the step were in the positive or negative direction depended on whether the first random number was greater or less than p_1. In like manner, the second random number determined the direction along θ.

Because step sizes were so small, the test-particle locations were not recorded every step. They were, instead, tallied at constant time increments $\Delta\tau$. Each time increment included $\Delta\tau\nu(V,\theta)$ steps. A count was kept of the number of times a test particle was found in each of the velocity zones (boxes). A large enough number of test particles A_{max} were walked to determine a velocity distribution. The time increments were selected so that usually no less than 10 nor more than 100 steps were taken between tallys. The number of $\Delta\tau$'s required to reach the loss cone was recorded to determine time of confinement and thus loss rate (appendix E).

After each set of A_{max} walks, new step size and probability matrices were determined with the test-particle distribution used as the field distribution. The elements of the tally matrix were reset to zero and the process repeated, if desired, for the $l + 1$ step of the iteration.

Numerous computations were made to explore the parameters of impact distance cutoff β, sample size A_{max}, and iteration index for suitable field convergence $l = l_{max}$. External conditions such as mirror ratio and injection distribution were selected either for reduction of computer time or for comparison of random-walk results with cases having analytical solutions.

RESULTS AND DISCUSSION

Influence of Impact Parameter

The scattering angles, thus step sizes, descriptive of Coulomb encounters are, in general, so small that even to evaluate the effect of β with a reasonable amount of computing time, required selection of very short walks. Short walks were obtained by using low mirror ratios ($B_c/B_o \approx 1$). The initial condition for this study was set to simulate injection of monoenergetic particles normal to the magnetic field $\theta = \pi/2$. Computations were carried out only for $l = 1$ and a Maxwellian field distribution.

A generalized parameter descriptive of the rate at which particles first reach prescribed conical boundaries in velocity space is plotted in figure 6. These boundaries (θ_c and $\pi - \theta_c$) were selected so that no set of (either 100 or 1000) particle walks took more than 15 minutes of computing time. At least three β values were used for each boundary condition. The mirror ratios (eq. (17)) became extremely close to one as b_{max} approached values representative of Debye lengths; in fact so low that these results have little direct application to mirror systems of interest. These results may be viewed as determining the average length of walk required to first reach a certain conical boundary in a Maxwellian field.

The regions of velocity space covered by the walks were so small that the step sizes and probabilities could be assumed constant over the length of the walks. This, in turn,

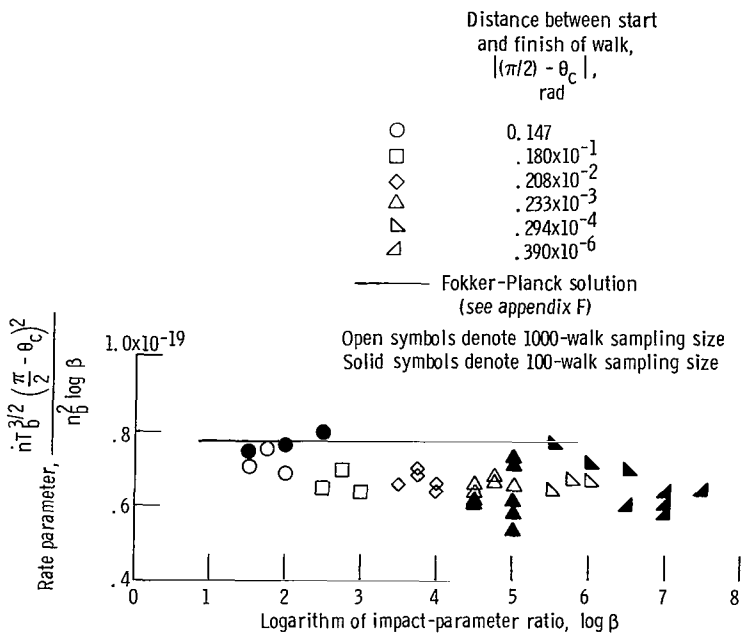

Figure 6. - Effect of impact-parameter cut-off distance on rate of reaching prescribed θ distance away from starting point at $\pi/2$. Singly charged particles of mass number 2; ratio of reference energy to field temperature, 15.

permitted an analytical solution of the Fokker-Planck equation (appendix F) which is shown by the line on figure 6.

This analysis gave the result that the loss-rate parameter

$$\frac{\dot{n} T_b^{3/2} \left(\frac{\pi}{2} - \theta_c\right)^2}{n_b^2 \log \beta}$$

was equal to a constant. This was verified over a range of β (from $10^{3/2}$ to $10^{15/2}$) by the computer results to within a spread of loss parameter of about 10 percent.

Some typical test-particle distributions are shown in figure 7. The marginal distribution in V

$$F_v(V) \equiv \frac{V^2 v_o^3}{n_b} \int_{\theta_c}^{\pi-\theta_c} f(\theta, v) \sin \theta \, d\theta = \int_{\theta_c}^{\pi-\theta_c} F(\theta, V) d\theta$$

is a delta function in the analysis. It is sharply peaked in the computer results, nearly all of the points plotted lying inside $0.998 \leq v/v_o \leq 1.002$. The marginal distribution in θ

$$F_\theta(\theta) \equiv \frac{\sin \theta}{n_b} \int_0^\infty f(\theta, v) v^2 \, dv = \int_0^\infty F(\theta, V) dV$$

for both the theory (appendix F) and the computer experiment can be represented by straight lines and agree well with each other.

The theoretical distribution from appendix F is

$$\left.\begin{aligned} F_\theta(\theta) = \frac{f_\theta(\theta)}{n_b} &= \frac{\theta - \theta_c}{\left(\frac{\pi}{2} - \theta_c\right)^2} && \text{when } \theta_c \leq \theta \leq \frac{\pi}{2} \\ &= \frac{1}{\frac{\pi}{2} - \theta_c} \left(1 + \frac{\frac{\pi}{2} - \theta}{\frac{\pi}{2} - \theta_c}\right) && \text{when } \frac{\pi}{2} \leq \theta \leq \pi - \theta_c \end{aligned}\right\} \quad (18)$$

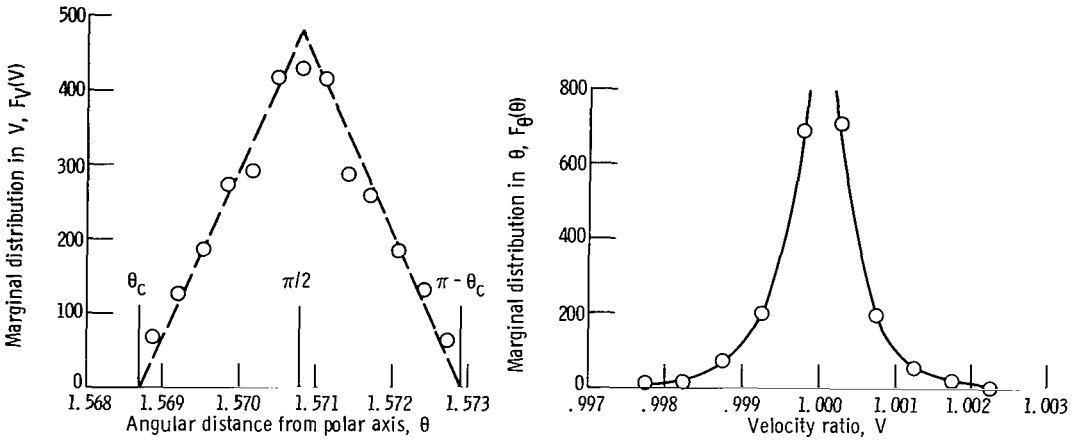

(a) Confined distribution.

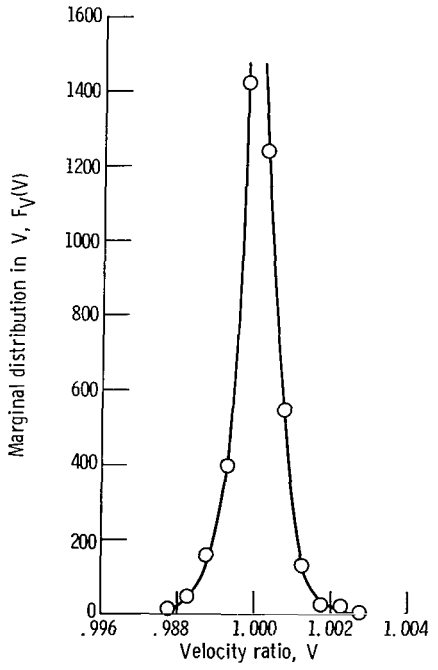

(b) Loss-cone distribution.

Figure 7. - Test-particle distribution for short walks and constant coefficients. Ratio of reference energy to field temperature, 15; sampling size, 1000; impact-parameter ratio, 10^4; distance between start and finish of walk, 0.00208 radian.

The theory and computer experiment appear to be in satisfactory agreement for purposes herein and encouraged applying the random-walk method to more complicated and practical models.

Comparison With the First-Order Solution of Budker

Analytical solution. - Among the very few analytical solutions of the Fokker-Planck equation applied to a magnetic mirror system is that of Budker (see refs. 5 and 19). This analysis makes the usual simplifying assumptions of appendix B plus the assumption of separability of the test-particle distribution functions; that is, it is assumed that

$$f(\theta, v) = f_\theta(\theta) f_v(v) \tag{19}$$

inside the mirror system, and that the injection distribution (source) function is

$$\dot{s}(\theta, v) = \dot{s}_\theta(\theta)\dot{s}_v(v)$$

Solutions are then sought where $f_v(v)$ is of the form $e^{-mv^2/2kT_b}$. For injection of particles perpendicular to the B field the solution of reference 5 is

$$f(\theta, v) = Ce^{-mv^2/2kT_b} \ln\left(\frac{\tan\frac{\theta}{2}}{\tan\frac{\theta_c}{2}}\right) \tag{20}$$

$$\dot{s}(\theta, v) = Ce^{-mv^2/2kT_b} \langle(\Delta\theta)^2\rangle \cos\theta_c \, \delta\left(\theta - \frac{\pi}{2}\right) \tag{21}$$

where the constant C can be used for normalizing. Results were reduced to this form by approximation of an integration over θ by the mean value theorem. The end-loss rate becomes

$$\dot{n} = \sqrt{\frac{2\pi}{m}} \frac{(Ze)^4 n_b^2 \ln\beta}{(4\pi\epsilon_o)^2 (kT)^{3/2}} \frac{3\ln\left(\sqrt{2}+1\right) - \sqrt{2}}{\left(\frac{1}{\sin\theta_c}\right)} \cos\theta_c$$

or

$$\frac{\dot{n}T^{3/2}\sqrt{m}}{Z^4 n_b^2 \log \beta} = 3.72\times10^{-31} \frac{\cos \theta_c}{\ln\left(\frac{B_c}{B_o}\right)} \tag{22}$$

In this solution the Fokker-Planck coefficients were based on a Maxwellian field distribution. It is thus like a first-order solution.

No energy gain or loss from the system was considered other than that added by the injection process or carried away with the escape of particles through the mirros. Thus the mean energy of the particles injected E_{inj} should equal the mean energy of the particles escaping for a steady-state solution. Integration of the product of equation (21) times $1/2\ mv^2$, and then division by $\dot{n}$ gives the mean energy per test particle to be

$$E_{inj} = 0.43\ kT_b$$

Thus the test particles are injected at a low energy to fill in the deficiency in velocity space due to the predominant escape of low-energy ions.

Random-walk solution. - Some preliminary insight into the random walk can be gained from inspection of the step sizes and probabilities of taking steps in the various directions. Step-size parameters for the V and θ components and for a Maxwellian field distribution are plotted in figure 5. Values used in a typical set of walks are given in a matrix form in the computer listings presented in appendix E.

For a given field distribution, path lines, as shown schematically on figure 1(b), can be envisioned. Use of the step sizes $\sqrt{\langle(\Delta V)^2\rangle/\nu}$ and $\sqrt{\langle(\Delta\theta)^2\rangle/\nu}$ from figure 5 permit study of the path lines for a Maxwellian field distribution. The magnitude of the slopes of such path lines increases with an increase of V because of the pronounced decrease of $\sqrt{\overline{(\Delta\theta)^2}}$ with V. It is apparent that the path line pattern is most conducive to the escape of particles at low V. It is in turn relatively easy for a particle in the high slope region to go to still higher velocities where escape is more difficult

The bias terms are equally important in the test-particle behavior. Entering into the bias term $(p_1 - q_1)$ in the V direction (eq. (4)) is a dynamic friction term $\overline{\Delta V}$. This term (discussed in ref. 7) is negative and tends to retard the test particle to zero mean velocity. Opposed to influence of $\overline{\Delta V}$ are the positive valued expressions

$$\frac{V}{2}\overline{(\Delta\theta)^2} + \frac{V \sin^2\theta}{2}\overline{(\Delta\varphi)^2} - \frac{1}{\nu}\frac{\partial\langle(\Delta V)^2\rangle}{\partial V}$$

which tend to diffuse the particles to the thinly populated regions of space at high V. In spherical coordinates the available volume in velocity space varies as V^2, making a large amount of room for particles at high V.

Similar terms appear in the $(p_2 - q_2)$ bias, which occurs in the θ direction. All terms except the last $(\sin\theta \cos\theta/2)\overline{(\Delta\varphi)^2}$, are zero for a Maxwellian field distribution. For higher order solutions ($l > 1$) the $\overline{\Delta\theta}$ and $-\overline{\Delta\theta\ \Delta V}/V$ terms tend to move test particles toward $\theta = \pi/2$. These terms thus help confine the particles. Opposed to this are the $-1/\nu(\partial\langle(\Delta\theta)^2\rangle/\partial\theta)$ and $[(\sin\theta \cos\theta)/2]\ \overline{(\Delta\varphi)^2}$ terms that make it easier for the particle to escape.

The initial locations of the test particles were determined by selection of random numbers from a distribution to simulate the injection velocity pattern of equation (20) as shown in appendix G. The walks were always started at the $\theta = \pi/2$.

Preliminary computer results verified that the test particles which were injected at low energies (according to eq. (21)) had a good chance of escaping with a relatively low number of steps. If, however, they remained inside the mirror system and by chance diffused to the high velocity region, their rate of escape was much reduced, even though the collision frequency was increased at high V. The test particles rush to such higher velocity zones at the expense of energy given up by the field particles. The field temperature was thus corrected for the energy exchanged with the appropriate test particle after each walk (appendix E).

Comparison of results. - Test-particle marginal distributions from the random-walk procedure are compared with the analytical results of reference 5 in figure 8. In general, the test particles distributed inside the mirror system in much the same pattern as predicted by reference 5 (figs. 8(a) and (b)) for the first-order results ($l = 1$). As the iteration process was continued, the test particles distributed in a slightly different pattern. The peak of the distribution shifted to a slightly higher V. Beyond a l of 2, however, changes were within a 10- to 20-percent scatter of the data for the usual sample size A_{max} of 500 particles. No attempt was made to optimize sample size against β. The parameter β was usually selected for completion of A_{max} times l_{max} walks in 20 minutes of computer time.

Starting the $l = 1$ calculation with the field-particle distribution in the θ direction cutoff at θ_c and $\pi - \theta_c$ appeared to give results as good as starting with a full Maxwellian distribution and completing the $l = 2$ step. By so doing the final number of steps in the iteration process (l_{max}) could be reduced by one.

The assumption of separability (eq. (19)) of the distribution function is often used to simplify analytical approaches (refs. 3, 5, and 19). This appears justified for the typi-

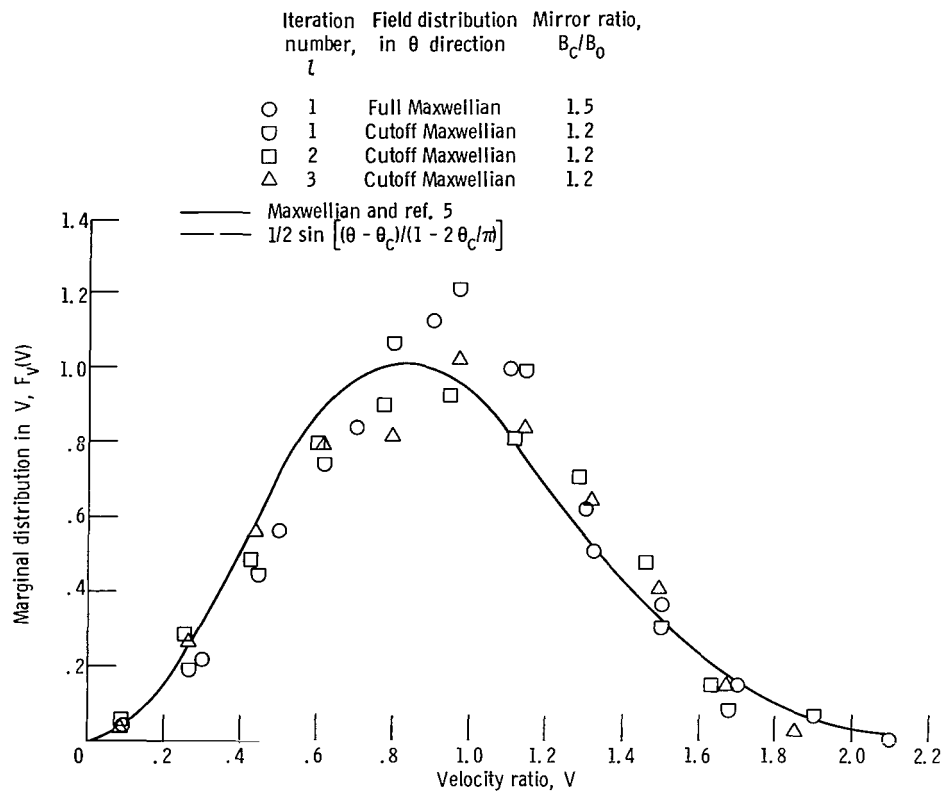

(a) Test-particle distribution in V direction.

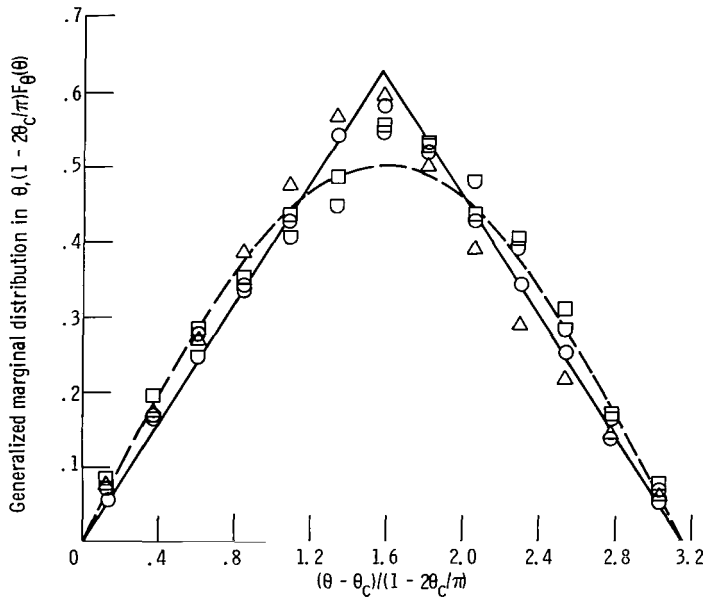

(b) Test-particle distribution in θ direction.

Figure 8. - Comparison of random-walk results with analysis of reference 5. Ratio of reference energy to field temperature, 1.5; sampling size, 500; atomic number, 1; impact-parameter ratio, $10^{5/2}$.

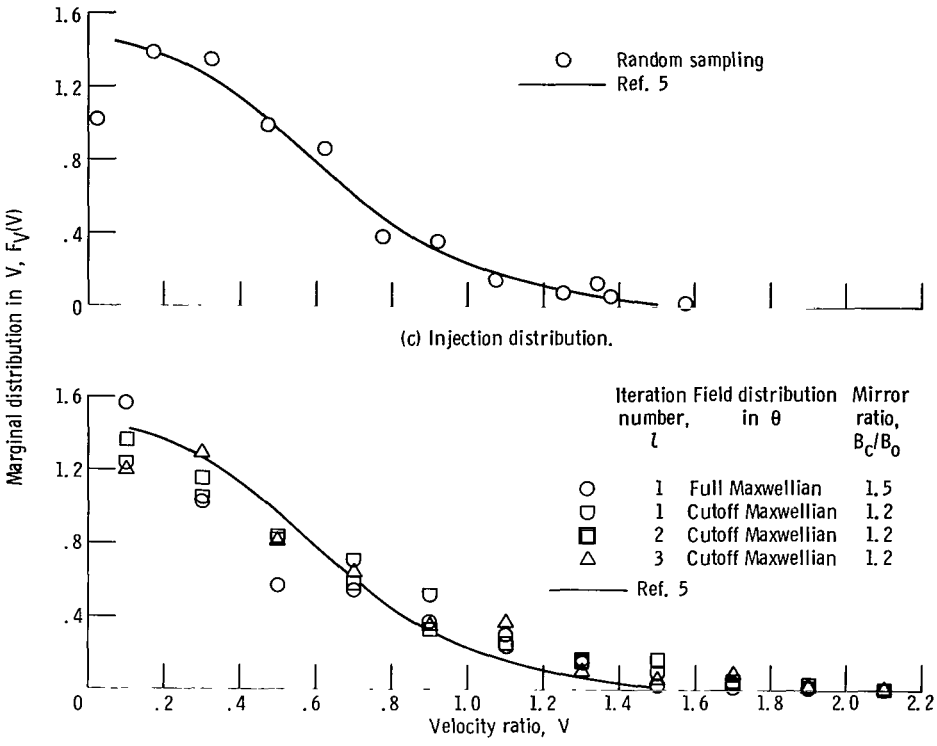

(c) Injection distribution.

(d) Distribution of particles as they first enter loss cone.

Figure 8. - Concluded.

cal set of data on figure 9. The open data points were obtained from the test-particle distributions of the random walk. These are a normalization of the KTJK(J,K) matrix (appendix E). The solid symbols denote the product of the random-walk marginal distributions in θ multiplied by the random-walk distributions in V. The lines are the analytical results of reference 5. The shift of the peaks of the computer results to values slightly higher than the analytical results is not due to the separability assumption. Good agreement is shown between the two studies for the outlet (loss cone) as well as for the inlet or injection distribution (figs. 8(c) and (d)). Thus the injection distributions of reference 5 appear quite satisfactory for a steady-state solution.

A comparison of the random-walk loss rates with the results of reference 5 is shown in figure 10. Agreement is close at a mirror ratio of 1.2. At higher mirror ratios, however, the loss-cone boundaries are extended enough that the chance of a particle walking to high V fields before escape is considerably improved, accounting in a large part for the reduction of loss rate with increase of B_c/B_o.

The rather steep decrease of loss rate with mirror ratio obtained from the random walks quite closely follows the $1/\log(B_c/B_o)$ trend predicted in references 3 and 13. The results of reference 5 differs by the inclusion of $\cos\theta_c$ in equation (22).

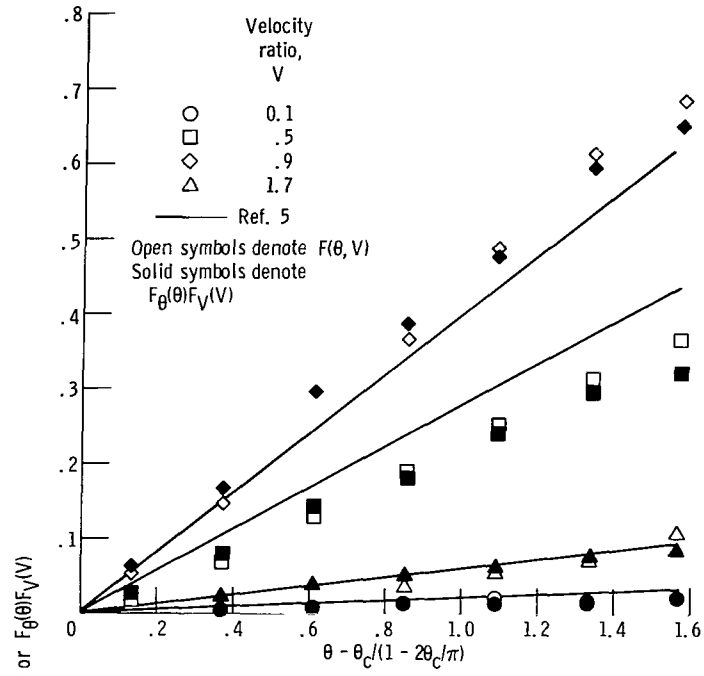

(a) Constant velocity ratio locations.

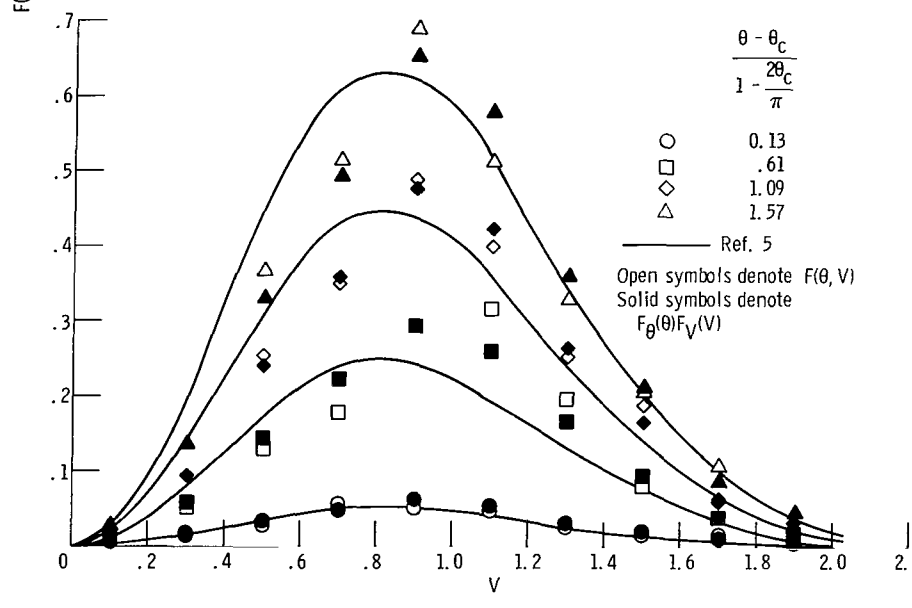

(b) Constant $\theta - \theta_c/(1 - 2\theta_c/\pi)$ locations.

Figure 9. - Study of separability of distribution. Sampling size, 500; ratio of reference energy to field temperature, 1.5; atomic number, 1; mirror ratio, 1.5; impact parameter ratio, $10^{5/2}$; iteration step number, 1.

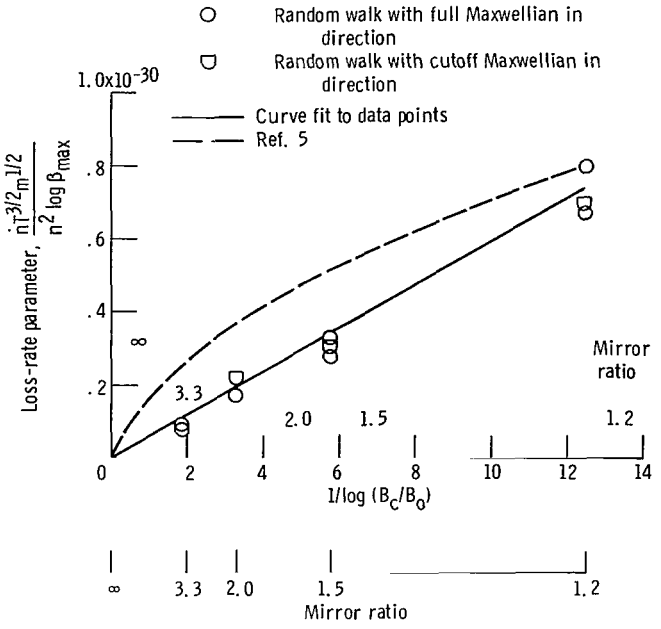

Figure 10. - Comparison of random-walk loss rates with the approximate analytical solution of reference 5.

The correction to the source term consisting of higher order terms in equation (8) was evaluated numerically for a Maxwellian field distribution. For this case, equation (8) reduces to

$$\dot{n}_{corrected} = \dot{n}_{random\ walk} - 0.003\times10^{-30} \frac{Z^4 n^2 \log \beta}{m^{1/2} T^{3/2}}$$

This correction, independent of mirror ratio is negligible in the random walk results on figure 11.

Computer time expenditure. - Each complete set of A_{max} walks and l steps in the iterative procedure required less than 20 minutes of computer execution time. It appears that this random-walk procedure could be extended to include special or time coordinates, or both, and work more general problems with reasonable computer time expenditure.

CONCLUSIONS

From a study of computer simulation of random walks of charged particles through ensembles of field particles inside magnetic mirror systems, and by comparison with results obtained from the Fokker-Planck equation for cases that could be solved analytically, the following conclusions were reached:

1. Computer time could be greatly reduced with no noticable reduction in accuracy

by a selective sampling of random numbers from the low impact-parameter range of the binary collisions used herein.

2. Test-particle distributions were insensitive to the assumed field-particle distributions.

3. The assumption of separability of the velocity distribution appears suitable for application to mirror system analyses.

4. End losses determined by the random-walk method were in close agreement with an approximate analytical solution of the Fokker-Planck equation at low mirror ratios. At higher mirror ratios the loss-cone boundaries increase permitting more test particles to reach the higher regions of velocity space where escape is much more difficult. The loss rate varies inversely as the logarithm of the reciprocal of the mirror ratio.

5. Each complete calculation, for a given set of initial and boundary conditions (injection velocity distribution and mirror ratio), was completed within 20 minutes of computer time. The study was limited to steady-state problems in velocity space. It appears that this random-walk procedure could be extended to include spatial or time coordinates (or both) with reasonable computer time.

Lewis Research Center,
National Aeronautics and Space Administration,
Cleveland, Ohio, October 20, 1969,
120-27.

APPENDIX A

SYMBOLS

[The International System of Units (SI) will be used throughout with the exception of temperature T, reported in keV, and the corresponding Boltzmann constant k, reported in J/keV.]

A	mass number
a	determinant of elements in metric tensor
a_{ij}	elements of metric tensor
a^{ij}	elements of cofactor of metric tensor
B	magnetic field
b	impact parameter
C	normalization constant
E	energy
E'_o	$mv_o^2/2k$
e	electric unit of charge
$F(\theta, V)$	normalized probability density times scale factors, $\frac{v_o v^2 \sin\theta}{n_b} f(v, \theta)$
$F_\theta(\theta)$	normalized marginal distribution in θ, $\int_0^\infty F(\theta, V)dv$
$F_V(V)$	normalized marginal distribution in V, $\int_0^{\pi-\theta_c} F(\theta, V)d\theta$
f	probability density
g	Rosenbluth potential = $\int f(\vec{v}_b)u\, d\vec{v}_b$
H	Heaviside unit function
h	Rosenbluth potential = $\int f(\vec{v}_b)\frac{1}{u} d\vec{v}_b$
k	Boltzmann constant = 1.6×10^{-16} J/keV
l	step number in iteration process
m	mass

N	number of dimensions
n	number density
$\dot{n}$	number of particles lost per unit time per unit volume of coordinate space
p_i	probability of 1 step in the positive direction along the i^{th} coordinate
q_i	probability of 1 step in the negative direction along the i^{th} coordinate
q^u	general curvilinear coordinate
$S^{\mu\nu}$	$\Gamma^{-1}\langle \Delta q^{\mu} \Delta q^{\nu} \rangle$
$\dot{s}$	number of particles injected per unit time per unit volume of phase space
r, R	random numbers
T	temperature
T^{μ}	$\Gamma^{-1}\langle \Delta q^{\mu} \rangle$
t	time
u	magnitude of relative velocity between a field and test particle
$u(\xi_1, \xi_2, \ldots, \xi_N)$	probability of particle being located at grid location $\xi_1, \xi_2, \ldots, \xi_N$
V	v/v_o
γ	random number
v	velocity
Y	some arbitrary collisionally dependent quality
Z	atomic number
β	impact-parameter ratio, b_{max}/b_{min}
Γ	interaction parameter, $= \dfrac{(Z_e)^4 \ln \beta}{4\pi\epsilon_o^2 m^2}$
δ	delta function, also used to denote finite difference
ϵ	azimuthal angle between orbital and fundamental collision planes
ϵ_o	capacitivity of vacuum

η number of components changed per encounter

θ angular distance from polar axis

ϑ_r angle between test and field-particle velocity vectors

ν collision frequency

ξ arbitrary coordinate in phase space

σ differential scattering cross section

φ azimuthal coordinate

Ω solid scattering angle

Subscripts:

b field particles

c collisional value, also used to denote loss cone or value at mirror location

e electron

inj injection

o reference value

Special symbols:

$\bar{}$ average per collision or per step

$\langle\rangle$ time average

APPENDIX B

TRANSFORMATION OF THE FOKKER-PLANCK EQUATION FROM RECTANGULAR CARTESIAN TO SPHERICAL COORDINATES

The Fokker-Planck equation can be written in rectangular Cartesian coordinates as

$$\left(\frac{\partial f}{\partial t}\right)_c = -\frac{\partial}{\partial v^\mu}\left(f\langle \Delta v^\mu \rangle\right) + \frac{1}{2}\frac{\partial^2}{\partial v^\mu \, \partial v^\nu}\left(f\langle \Delta v^\mu \, \Delta v^\nu \rangle\right)$$

Superscripts are used in this appendix to denote component direction, leaving subscripts to denote covariant differentiation. Summation convention of repeated indices will be used. The subscript c on $\partial f/\partial t$ means changes of f due to collisions.

Following the procedure of appendix IV of reference 11, this equation can be written in covariant form as

$$\Gamma^{-1}\left(\frac{\partial f}{\partial t}\right)_c = -(fT^\mu)_{,\,\mu} + \frac{1}{2}(fS^{\mu\nu})_{,\,\mu\nu}$$

which is valid for any set of curvilinear coordinates, q^1, q^2, q^3.

The quantity Γ is an interaction parameter,

$$T^\mu = a^{\mu\nu}(h_{,\,\nu}) = \langle \Delta q^\mu \rangle \Gamma^{-1} \tag{B1}$$

and

$$S^{\mu\nu} = a^{\mu\omega}a^{\nu\tau}(g_{,\,\omega\tau}) = \langle \Delta q^\mu \, \Delta q^\nu \rangle \Gamma^{-1} \tag{B2}$$

The terms $\Gamma S^{\mu\nu}$ are dispersion coefficients, and ΓT^μ is related to dynamic friction.

For spherical coordinates $q^1 = v$, $q^2 = \theta$, and $q^3 = \varphi$. The elements of the metric tensor are

$$a_{11} = 1$$

$$a_{22} = v^2$$

$$a_{33} = v^2 \sin^2\theta$$

$$a_{\mu\nu} = 0 \qquad \text{if} \quad \mu \neq \nu$$

and the elements of its conjugate are

$$a^{11} = 1$$

$$a^{22} = \frac{1}{v^2}$$

$$a^{33} = \frac{1}{v^2 \sin^2\theta}$$

$$a^{\mu\nu} = 0 \qquad \text{if} \quad \mu \neq \nu$$

By the procedure of covariant differentiation

$$(fT^{\mu})_{,\,\mu} = \frac{\partial fT^{\mu}}{\partial q^{\mu}} + \left\{ \begin{matrix} \mu \\ \alpha\mu \end{matrix} \right\} (fT^{\alpha}) = \frac{1}{\sqrt{a}} \frac{\partial}{\partial q^{\mu}} \left(\sqrt{a}\, fT^{\mu} \right)$$

where the Christoffel symbol $\left\{ \begin{matrix} \mu \\ \alpha\mu \end{matrix} \right\}$ with repeated indices equals $\frac{1}{\sqrt{a}} \frac{\partial \sqrt{a}}{\partial q^{\alpha}}$ and a is the determinant of the matrix of elements $a_{\mu\nu}$. For spherical coordinates

$$a = v^4 \sin^2\theta$$

Thus,

$$\Gamma(fT^{\mu})_{,\,\mu} = \frac{1}{v^2} \frac{\partial}{\partial v} (v^2 f\langle \Delta v \rangle) + \frac{1}{\sin\theta} \frac{\partial}{\partial \theta} (f \sin\theta \langle \Delta\theta \rangle) + \frac{\partial}{\partial \varphi} (f\langle \Delta\varphi \rangle)$$

In like manner

$$\Gamma(fS^{\mu\nu})_{,\,\mu\nu} = \frac{1}{\sqrt{a}} \frac{\partial^2 \left(\sqrt{a}\, fS^{\mu\nu} \right)}{\partial q^{\mu}\, \partial q^{\nu}} + \frac{1}{\sqrt{a}} \frac{\partial}{\partial q^{\nu}} \left(\sqrt{a} \left\{ \begin{matrix} \nu \\ \omega\mu \end{matrix} \right\} fS^{\mu\omega} \right)$$

and for spherical coordinates

$$\frac{\partial}{\partial q^\nu}\left(\sqrt{a}\left\{\begin{matrix}\nu\\ \omega\mu\end{matrix}\right\} f S^{\mu\omega}\right) = \frac{\partial}{\partial q^\nu}\left[v^2 \sin\theta\, f S^{\mu\omega}\, \frac{a^{\nu\nu}}{2}\left(\frac{\partial a_{\omega\nu}}{\partial q^\mu} + \frac{\partial a_{\mu\nu}}{\partial q^\omega} - \frac{\partial a_{\omega\mu}}{\partial q^\nu}\right)\right]$$

$$= -\frac{\partial}{\partial v}\left[v^2 \sin\theta\, f(v S^{22} + v \sin^2\theta S^{33})\right] + \frac{\partial}{\partial\theta}\left[\sin\theta\, f(2v S^{12} - v^2 \sin\theta\cos\theta\, S^{33})\right]$$

$$+ \frac{\partial}{\partial\varphi}\left[2fv(\sin\theta\, S^{13} + v\cos\theta\, S^{23})\right]$$

where use is made of the symmetry of $S^{\mu\nu}$. Finally the Fokker-Planck equation in spherical coordinates becomes

$$\left(\frac{\partial f}{\partial t}\right)_c = -\frac{1}{v^2}\frac{\partial}{\partial v}(v^2 f\langle\Delta v\rangle) - \frac{1}{\sin\theta}\frac{\partial}{\partial\theta}(f\sin\theta\langle\Delta\theta\rangle) - \frac{\partial}{\partial\varphi}(f\langle\Delta\varphi\rangle) + \frac{1}{2v^2}\frac{\partial^2 v^2 f\langle(\Delta v)^2\rangle}{\partial v^2} + \frac{1}{2\sin\theta}\frac{\partial^2 f\sin\theta\langle(\Delta\theta)^2\rangle}{\partial\theta^2}$$

$$+\frac{1}{2}\frac{\partial^2 f\langle(\Delta\varphi)^2\rangle}{\partial\varphi^2} + \frac{1}{v^2\sin\theta}\frac{\partial^2}{\partial v\,\partial\theta}(v^2\sin\theta f\langle\Delta v\,\Delta\theta\rangle) + \frac{1}{v^2}\frac{\partial}{\partial v\,\partial\varphi}(v^2 f\langle\Delta v\,\Delta\varphi\rangle) + \frac{1}{\sin\theta}\frac{\partial}{\partial\theta\,\partial\varphi}(\sin\theta f\langle\Delta\theta\,\Delta\varphi\rangle)$$

$$-\frac{1}{2v^2}\frac{\partial}{\partial v}\left[v^3 f\left(\langle(\Delta\theta)^2\rangle + \sin^2\theta\langle(\Delta\varphi)^2\rangle\right)\right] + \frac{1}{2v\sin\theta}\frac{\partial}{\partial\theta}\left[f\sin\theta\left(2\langle\Delta\theta\,\Delta v\rangle - v\sin\theta\cos\theta\langle(\Delta\varphi)^2\rangle\right)\right] \qquad \text{(B3)}$$

$$+\frac{1}{v}\frac{\partial}{\partial\varphi}\left[f\left(\langle\Delta v\,\Delta\varphi\rangle + \frac{v\cos\theta}{\sin\theta}\langle\Delta\theta\,\Delta\varphi\rangle\right)\right]$$

APPENDIX C

PHYSICAL MODEL OF MAGNETIC MIRROR SYSTEM

The physical model to which this analysis is applied is the usual simplified one, well described in many references; such as, for example, pages 186 to 189 of reference 5, pages 3 to 5 of reference 13, pages 2 and 3 of reference 3, and pages 7 to 9 of reference 17. In essence, the magnetic mirror system provides a long cylindrical region of uniform magnetic field (fig. 3). The mirror regions are assumed to be relatively short so that essentially all the Coulomb scattering occurs in the central region. Only binary collisions and classical particles will be considered.

Once a particle enters the loss cone in velocity space, no matter where it is in physical or coordinate space, it is assumed lost from the system. Only scattering of ions off other ions is considered. Thus electrons serve only as a neutralizing and shielding background of particles. For study herein, no macroscopic electric field will be accounted for except possibly as a boundary condition in the manner of reference 20.

The radius of the confining field must obviously be much larger than the ion cyclotron radius. This can be accomplished by suitable magnitude of the B field. The azimuthal symmetry of the B field makes $\vec{v} \times \vec{B} \cdot \nabla_v f \equiv 0$ as shown in appendix A-1 of reference 13.

These assumptions culminate in the elimination of the gradient terms, in velocity as well as in coordinate space, from the Boltzmann equation. The Boltzmann equation thus reduces to

$$\frac{\partial f}{\partial t} = \left(\frac{\partial f}{\partial t}\right)_c + \dot{s}$$

where $(\partial f/\partial t)_c$ is the change of f due to collisions, usually determined by the Fokker-Planck equation, and $\dot{s}$ represents a sink density in velocity space, uniform in coordinate space.

APPENDIX D

FOKKER-PLANCK AND RANDOM-WALK COEFFICIENTS IN SPHERICAL COORDINATES

The Fokker-Planck coefficients are time averages of various first- and second-order increments of velocity due to collisions. The random-walk process, in turn, requires the average per collision of these same velocity increments. The two types of averages, denoted by the angular brackets and bar notations, respectively, differ by the collision frequency ν. Thus only one set of coefficients and the collision frequency need be derived for the physical conditions of interest.

The time rate of change of some collisionally dependent quantity Y averaged over all scattering angles and all velocities of the scattering (field) particles is

$$\langle Y \rangle = \int f_b(\vec{v}_b) \int Yu\sigma(u, \Omega) d\Omega \, d\vec{v}_b \tag{D1}$$

where the subscript b refers to field particles, and σ is the differential cross section of scattering over the solid angle Ω. The magnitude of the relative velocity between a test-particle of velocity $\vec{v}$ and a field particle of velocity $\vec{v}_b$ is

$$u = \sqrt{v^2 + v_b^2 - 2vv_b \cos \vartheta_r} \tag{D2}$$

where ϑ_r is the angle between $\vec{v}$ and $\vec{v}_b$. The distribution function of field particles is denoted by f_b and is normalized so that

$$\int f(\vec{v}_b) d\vec{v}_b = n_b$$

Using Rosenbluth potential (ref. 11) defined as

$$h = \int f(\vec{v}_b) \frac{1}{u} \, d\vec{v}_b$$

and

$$g = \int f(\vec{v}_b) u \, d\vec{v}_b$$

and letting Y equal the i^{th} component of $\Delta\vec{v}$ yields (ref. 11)

$$\langle \Delta v^i \rangle = \Gamma \frac{\partial h}{\partial v^i} \qquad i = 1,\ 2,\ 3,$$

the covariant form of which is given by equation (B1)

$$\langle \Delta q^\mu \rangle = \Gamma a^{\mu\nu}(h_{,\nu})$$

For Coulomb encounters

$$\Gamma = \frac{Z^4 e^4 \ln \beta}{4\pi\epsilon_o^2 m^2} \tag{D3}$$

where β is the ratio of the maximum impact parameter b_{max} to minimum, b_{min}. When Y is set equal to the product $\Delta v^i\, \Delta v^j$, it follows that (ref. 11)

$$\langle \Delta v^i\, \Delta v^j \rangle = \Gamma \frac{\partial^2 g}{\partial v^i\, \partial v^j} \qquad i, j = 1,\ 2,\ 3$$

and the covariant form is given by equation (B2) as

$$\langle \Delta q^\mu\, \Delta q^\nu \rangle = \Gamma a^{\mu\omega} a^{\nu\tau}(g_{,\omega\tau})$$

When Y = 1, it is apparent from equation (D1) that the collision frequency is obtained. Using the well known scattering relation involving solid angle Ω, impact parameter b, and azimuthal angle ϵ

$$\sigma(\Omega)d\Omega = b\ db\ d\epsilon$$

in (D1) gives

$$\nu = \pi\left(b_{max}^2 - b_{min}^2\right)g$$

which is an invariant and independent of the coordinate system. In spherical coordinates, the coefficients of main interest are

$$\langle \Delta v \rangle = \Gamma \frac{\partial h}{\partial v}$$

$$\langle \Delta \theta \rangle = \frac{\Gamma}{v^2} \frac{\partial h}{\partial \theta}$$

$$\langle \Delta \varphi \rangle = \frac{\Gamma}{v^2 \sin^2 \theta} \frac{\partial h}{\partial \varphi}$$

$$\langle \Delta \theta \, \Delta v \rangle = \frac{\Gamma}{v^2} \left(\frac{\partial^2 g}{\partial \theta \, \partial v} - \frac{1}{v} \frac{\partial g}{\partial \theta} \right)$$

$$\langle (\Delta v)^2 \rangle = \Gamma \frac{\partial^2 g}{\partial v^2}$$

$$\langle (\Delta \theta)^2 \rangle = \frac{\Gamma}{v^4} \left(\frac{\partial^2 g}{\partial \theta^2} + v \frac{\partial g}{\partial v} \right)$$

$$\langle (\Delta \varphi)^2 \rangle = \frac{\Gamma}{v^4 \sin^4 \theta} \left(\frac{\partial^2 g}{\partial \varphi^2} + v \sin^2 \theta \frac{\partial g}{\partial v} + \sin \theta \cos \theta \frac{\partial g}{\partial \theta} \right)$$

$$\langle \Delta v \, \Delta \varphi \rangle = \frac{\Gamma}{v^2 \sin^2 \theta} \left(\frac{\partial^2 g}{\partial v \, \partial \varphi} - \frac{1}{v} \frac{\partial g}{\partial \varphi} \right)$$

$$\langle \Delta \theta \, \Delta \varphi \rangle = \frac{\Gamma}{v^4 \sin^2 \theta} \left(\frac{\partial^2 g}{\partial \theta \, \partial \varphi} - \frac{\cos \theta}{\sin \theta} \frac{\partial g}{\partial \varphi} \right)$$

These expressions can be reduced one step further without specifying f_b since differentiation is with respect to the coordinates of the test particles.

Azimuthal symmetry. - For aximuthal symmetry $\partial/\partial\varphi$ is zero and thus $\langle \Delta\varphi \rangle$, $\langle \Delta v \, \Delta\varphi \rangle$, $\langle \Delta\theta \, \Delta\varphi \rangle$ are zero. The remaining expressions are reduced as follows: Using

$$\cos \vartheta_r = \cos \theta \cos \theta_b + \sin \theta \sin \theta_b \cos(\varphi - \varphi_b)$$

and differentiating under the integral sign gives

$$\langle \Delta v \rangle = -2\Gamma \int \frac{v - v_b \cos \vartheta_r}{\left(v^2 + v_b^2 - 2vv_b \cos \vartheta_r\right)^{3/2}} f(\vec{v}_b) d\vec{v}_b \tag{9a}$$

$$\langle \Delta \theta \rangle = -\frac{2\Gamma}{v^2} \int vv_b \frac{\left[\sin \theta \cos \theta_b - \cos \theta \sin \theta_b \cos(\varphi - \varphi_b)\right]}{\left(v^2 + v_b^2 - 2vv_b \cos \vartheta_r\right)^{3/2}} f(\vec{v}_b) d\vec{v}_b \tag{9b}$$

$$\langle \Delta \theta \, \Delta v \rangle = \frac{\Gamma}{v^2} \int vv_b (v - v_b \cos \vartheta_r) \frac{\left[\sin \theta \cos \theta_b - \cos \theta \sin \theta_b \cos(\varphi - \varphi_b)\right]}{\left(v^2 + v_b^2 - 2vv_b \cos \vartheta_r\right)^{3/2}} f(\vec{v}_b) d\vec{v}_b \tag{9c}$$

$$\langle (\Delta v)^2 \rangle = \Gamma \int \frac{1}{\left(v^2 + v_b^2 - 2vv_b \cos \vartheta_r\right)^{1/2}} - \frac{(v - v_b \cos \vartheta_r)^2}{\left(v^2 + v_b^2 - 2vv_b \cos \vartheta_r\right)^{3/2}} f(\vec{v}_b) d\vec{v}_b \tag{9d}$$

$$\langle (\Delta \theta)^2 \rangle = \frac{\Gamma}{v^4} \int \left\{ \frac{v^2}{\left(v^2 + v_b^2 - 2vv_b \cos \vartheta_r\right)^{1/2}} - \frac{v^2 v_b^2 \left[\sin \theta \cos \theta_b - \cos \theta \sin \theta_b \cos(\varphi - \varphi_b)\right]^2}{\left(v^2 + v_b^2 - 2vv_b \cos \vartheta_r\right)^{3/2}} \right\} f(\vec{v}_b) d\vec{v}_b \tag{9e}$$

$$\langle (\Delta \varphi)^2 \rangle = \frac{\Gamma}{v^4 \sin^2 \theta} \int \frac{v^2 - vv_b \sin \theta_b \cos(\varphi - \varphi_b)}{\left(v^2 + v_b^2 - 2vv_b \cos \vartheta_r\right)^{1/2}} f(\vec{v}_b) d\vec{v}_b \tag{9f}$$

$$\nu = \frac{4\Gamma\beta^2}{9 \ln \beta} \left(\frac{m}{2kT_b}\right)^2 \int \left(v^2 + v_b^2 - 2vv_b \cos \vartheta_r\right)^{1/2} f(\vec{v}_b) d\vec{v}_b \tag{9g}$$

where b_{min} was set equal to the classical distance of closest approach

$$b_{min} = \frac{(Ze)^2}{4\pi\epsilon_o\left(\frac{3}{2}kT_b\right)} = \frac{(Ze)^2}{6\pi\epsilon_o kT_b}$$

The average value of these quantities per collision, in dimensionless form, are

$$\Delta\bar{V} = \frac{\langle\Delta V\rangle}{\nu} = -\frac{9}{2}\frac{\ln\beta}{\beta^2}\left(\frac{T_b}{E'_o}\right)^2 \frac{\int \frac{V - V_b\cos\vartheta_r}{\left(V^2 + V_b^2 - 2VV_b\cos\vartheta_r\right)^{3/2}} f(\vec{V}_b)d\vec{V}_b}{\int\sqrt{V^2 + V_b^2 - 2VV_b\cos\vartheta_r}\, f(\vec{V}_b)d\vec{V}_b} \tag{D4a}$$

$$\Delta\dot{\theta} = \frac{\langle\Delta\theta\rangle}{\nu} = -\frac{9}{2}\frac{\ln\beta}{V^2\beta^2}\left(\frac{T_b}{E'_o}\right)^2 \frac{\int \frac{VV_b\left[\sin\theta\cos\theta_b - \cos\theta\sin\theta_b\cos(\varphi - \varphi_b)\right]}{\left(V^2 + V_b^2 - 2VV_b\cos\vartheta_r\right)^{3/2}} f(\vec{V}_b)d\vec{V}_b}{\int\sqrt{V^2 + V_b^2 - 2VV_b\cos\vartheta_r}\, f(\vec{V}_b)d\vec{V}_b} \tag{D4b}$$

$$\overline{\Delta\theta\,\Delta V} = \frac{\langle\Delta\theta\,\Delta V\rangle}{\nu} = \frac{9}{4}\frac{\ln\beta}{\beta^2 V^2}\left(\frac{T_b}{E'_o}\right)^2 \frac{\int \frac{VV_b(V - V_b\cos\vartheta_r)\left[\sin\theta\cos\theta_b - \cos\theta\sin\theta_b\cos(\varphi - \varphi_b)\right]}{\left(V^2 + V_b^2 - 2VV_b\cos\vartheta_r\right)^{3/2}} f(\vec{V}_b)d\vec{V}_b}{\int\sqrt{V^2 + V_b^2 - 2VV_b\cos\vartheta_r}\, f(\vec{V}_b)d\vec{V}_b} \tag{D4c}$$

$$(\Delta V)^2 = \frac{\langle(\Delta V)^2\rangle}{\nu} = \frac{9}{4}\frac{\ln\beta}{\beta^2}\left(\frac{T_b}{E'_o}\right)^2 \frac{\int\left[\frac{1}{\sqrt{V^2 + V_b^2 - 2VV_b\cos\vartheta_r}} - \frac{(V - V_b\cos\vartheta_r)^2}{\left(V^2 + V_b^2 - 2VV_b\cos\vartheta_r\right)^{3/2}}\right] f(\vec{V}_b)d\vec{V}_b}{\int\sqrt{V^2 + V_b^2 - 2VV_b\cos\vartheta_r}\, f(\vec{V}_b)d\vec{V}_b} \tag{D4d}$$

$$\overline{(\Delta\theta)^2} = \frac{\langle(\Delta\theta)^2\rangle}{\nu}$$

$$= \frac{9}{4}\frac{\ln\beta}{V^4\beta^2}\left(\frac{T_b}{E'_o}\right)^2 \frac{\int\left\{\frac{V^2}{\sqrt{V^2 + V^2 - 2VV_b\cos\vartheta_r}} - \frac{V^2V_b^2\left[\sin\theta\sin\theta_b - \cos\theta\cos\theta_b\cos(\varphi - \varphi_b)\right]^2}{\left(V^2 + V_b^2 - 2VV_b\cos\vartheta_r\right)^{3/2}}\right\} f(\vec{V}_b)d\vec{V}_b}{\int\sqrt{V^2 + V_b^2 - 2VV_b\cos\vartheta_r}\, f(\vec{V}_b)d\vec{V}_b} \tag{D4e}$$

$$\overline{(\Delta\varphi)^2} = \frac{\langle(\Delta\varphi)^2\rangle}{\nu} = \frac{9}{4}\,\frac{\ln\beta\left(\frac{T_b}{E'_o}\right)^2}{V^4\beta^2\sin^2\theta}\,\frac{\int\left[V^2 - VV_b\left(\frac{\sin\theta\sin\theta_b + \cos^2\theta\sin\theta_b}{\sin\theta}\right)\cos(\varphi - \varphi_b)\right]\sqrt{V^2 + V_b^2 - 2VV_b\cos\vartheta_r}\,f(\vec{V}_b)d\vec{V}_b}{\int\sqrt{V^2 + V_b^2 - 2VV_b\cos\vartheta_r}\,f(\vec{V}_b)d\vec{V}_b} \qquad \text{(D4f)}$$

and

$$\nu = \frac{4\Gamma\beta^2}{9\ln\beta}\left(\frac{m}{2kT}\right)^{3/2}\left(\frac{E'_o}{T_b}\right)^{1/2}\int\sqrt{V^2 + V_b^2 - 2VV_b\cos\vartheta_r}\,f(\vec{V}_b)\,d\vec{V}_b \qquad \text{(D4g)}$$

where

$$V = \frac{v}{v_o} \qquad V_b = \frac{v_b}{v_o} \qquad E_o = \frac{1}{2}mv_o^2 = kE'_o \qquad \beta >> 1. \qquad \text{(D5)}$$

Maxwellian distribution. - A popular simplifying assumption is that the field particles are distributed in a Maxwellian spherical distribution. This a case of the "diffusion approximation" on page 175 of reference 5 and corresponds to the use of "effective Rosenbluth potentials" as on page 15 of reference 19. With this assumption

$$f_b\,dv_b = n_b\left(\frac{m}{2\pi kT_b}\right)^{3/2} v_b^2\,e^{-mv_b^2/2kT_b}\sin\theta_b\,d\theta_b\,d\varphi_b\,dv_b \qquad (10)$$

For a spherical distribution, ϑ_r can be replaced by θ_b. Integrating between the limits

$$0 \le v_b \le \infty$$

$$0 \le \theta_b \le \pi$$

and

$$0 \le \varphi_b \le 2\pi$$

gives

$$g = g(v) = n_b\left[\sqrt{\frac{2kT_b}{\pi m}}\, e^{-mv^2/2kT_b} + \left(v + \frac{kT_b}{mv}\right)\mathrm{erf}\left(\sqrt{\frac{m}{2kT}}\, v\right)\right]$$

The remaining potential h can be obtained from

$$h = \nabla_v^2 g = \frac{2n_b}{v}\,\mathrm{erf}\left(\sqrt{\frac{m}{2kT_b}}\, v\right)$$

Since both g and h are independent of θ and φ, it is apparent from (B1) and (B2) that

$$\langle \Delta\theta \rangle = \langle \Delta\varphi \rangle = \langle \Delta\theta\, \Delta v \rangle \equiv 0$$

The remaining terms of interest for this field distribution are

$$\langle \Delta v \rangle = \frac{2n_b \Gamma}{v^2}\left[2\sqrt{\frac{m}{2\pi kT_b}}\, v e^{-mv^2/2kT_b} - \mathrm{erf}\left(\sqrt{\frac{m}{2kT_b}}\, v\right)\right] \tag{11a}$$

$$\langle (\Delta v)^2 \rangle = -\frac{kT_b}{mv}\langle \Delta v \rangle \tag{11b}$$

$$\langle (\Delta\theta)^2 \rangle = \frac{n_b \Gamma}{v^3}\sqrt{\frac{2kT_b}{\pi m}}\,\frac{1}{v} e^{-mv^2/2kT_b} + \left(1 - \frac{kT_b}{mv^2}\right)\mathrm{erf}\left(\sqrt{\frac{m}{2kT_b}}\, v\right) \tag{11c}$$

$$\langle (\Delta\varphi)^2 \rangle = \frac{1}{\sin^2\theta}\langle (\Delta\theta)^2 \rangle \tag{11d}$$

and

$$\nu = \frac{4n_b(\beta^2 - 1)}{9 \ln \beta}\left(\frac{m}{2kT_b}\right)^2 v\Gamma\left[\sqrt{\frac{2kT_b}{\pi m}}\,\frac{1}{v} e^{-mv^2/2kT_b} + \left(1 + \frac{kT_b}{mv^2}\right)\mathrm{erf}\left(\sqrt{\frac{m}{2kT_b}}\, v\right)\right] \tag{11e}$$

These expressions for $\langle \Delta v \rangle$ and $\langle (\Delta v)^2 \rangle$ agree with those of reference 5 and with those of Chandrasekhar (pp. 73 to 75 of ref. 12). These coefficients are called parallel components since they are changes in v in a direction parallel to v. Agreement with these references is also obtained for the perpendicular component of diffusion which is

$$\langle (\Delta v_\perp)^2 \rangle = v^2 \left[\langle (\Delta\theta)^2 \rangle + \sin^2\theta \langle (\Delta\varphi)^2 \rangle \right]$$

Remaining quantities of interest are

$$\overline{\Delta V} = \frac{\langle \Delta V \rangle}{\nu} = + \frac{9}{2} \frac{\ln \beta}{\beta^2} \left(\frac{T_b}{E'_o} \right)^2 \frac{\left[2V \sqrt{\frac{E'_o}{\pi T_b}}\, e^{-V^2 E'_o / T_b} - \operatorname{erf}\left(V \sqrt{\frac{E'_o}{T_b}} \right) \right]}{V^3 \left[\frac{1}{V} \sqrt{\frac{T_b}{\pi E'_o}}\, e^{-V^2 E'_o / T_b} + \left(1 + \frac{T_b}{2V^2 E'_o} \right) \operatorname{erf}\left(V \sqrt{\frac{E'_o}{T_b}} \right) \right]} \tag{15a}$$

$$\overline{(\Delta V)^2} = - \frac{T_b}{2VE'_o}\, \overline{\Delta V} \tag{15b}$$

$$\overline{(\Delta\theta)^2} = \frac{\langle (\Delta\theta)^2 \rangle}{\nu} = \frac{9}{4} \frac{\ln \beta}{V^4 \beta^2} \left(\frac{T_b}{E'_o} \right)^2 \frac{\left[\frac{1}{V} \sqrt{\frac{T_b}{\pi E'_o}}\, e^{-V^2 E'_o / T_b} + \left(1 - \frac{T_b}{2VE'_o} \right) \operatorname{erf}\left(V \sqrt{\frac{E'_o}{T_b}} \right) \right]}{\left[\frac{1}{V} \sqrt{\frac{T_b}{\pi E'_o}}\, e^{-V^2 E'_o / T_b} + \left(1 + \frac{T_b}{2VE'_o} \right) \operatorname{erf}\left(V \sqrt{\frac{E'_o}{T_b}} \right) \right]} \tag{15c}$$

$$\overline{(\Delta\varphi)^2} = \frac{1}{\sin^2\theta}\, \overline{(\Delta\theta)^2} \tag{15d}$$

and

$$\nu = \frac{0.518 \times 10^{-31}\, n_b Z^4 \beta^2 V}{T_b^{3/2} m^{1/2}} \sqrt{\frac{E'_o}{T_b}} \left[\left(1 + \frac{T_b}{2V^2 E'_o} \right) \operatorname{erf}\left(V \sqrt{\frac{E'_o}{T_b}} \right) + \frac{1}{V} \sqrt{\frac{T_b}{\pi E'_o}}\, e^{-E'_o V^2 / T_b} \right] \tag{15e}$$

where $B >> 1$.

APPENDIX E

DESCRIPTION OF COMPUTING PROCEDURE

A flow chart representing a typical calculation procedure is given in figure 11. The corresponding FORTRAN program and some typical results are included at the end of this appendix. This is preceded by a key to the computer words. A brief description of the program to perform the random walk studies is given in the following discussion.

The distribution of field particles is represented by KTJK(J, K) matrices. The indices J and K represent partitions in V and θ, respectively. In most of the computations this was an 11 by 13 matrix, thus dividing the velocity space of most importance into 143 zones. The initial (LL=1) field distribution was read from data cards.

The velocity field to which the test particles had access was also divided into zones. These zones were identified by subscripts M and L. Step sizes, DVSQAV(M, L) and DXSQAV(M, L), and probabilities, TWOP(M, L) and TWOR(M, L), were computed over the ranges of M and L for the field distribution specified by the KTJK matrix. Integration of equations (9) with respect to φ was by Gaussian quadratures. Integrations with respect to V and θ, weighted by $v^2 \sin\theta\, f(v, \theta)$ as in equations (9), were replaced by summations over the J and K indices with weighting by KTJK(J, K).

Because step sizes are so small, the test-particle locations were only recorded every MMAX(M, L) steps. To obtain steady-state distributions, it is desired to locate the test particle after each small constant increment of time, $\Delta\tau$. The number of steps per constant increment of time is

$$\mathrm{RMAX(M, L)} = \frac{(\mathrm{RMAX1})(\nu(\mathrm{M, L}))}{\nu(\mathrm{V2=1,\ X2=\pi/2})} \tag{E1}$$

where RMAX is the real number counterpart of integer MMAX. The value of RMAX1 is specified at the beginning of the program and should be judiciously selected to keep computing time down and yet obtain accuracy.

An alternate procedure to the use of velocity zones and matrix descriptions when LL=1 was to specify a Maxwellian distribution of field particles and use equations (15). In this way the step sizes, probabilities, and number of steps per time increment are continuous functions of test-particle location and are integrated over a continuous field distribution. A comparison of this procedure with the matrix procedure served as a check on the required number of velocity zones for sufficient accuracy in the matrix representation. Excellent agreement was obtained by use of the 11 by 13 matrices. Suitable values of RMAX1 varied from 10 to 10^3 depending primarily on β.

The test particles were labeled by A (used as an integer). It was found that the

walks of about 500 test particles (AMAX=500) was required for a representative sample.

The initial conditions for the random walks depended on the injection distribution being simulated. For the example on the flow chart, V2 was always set at 1.0 and X2 at $\pi/2$, representative of monoenergetic injection and normal to B field. This initial condition was used in the short walk calculations. For simulating the injection distribution of reference 5, the procedure of appendix G was used.

The random-walk proper comprised a small part of the programming effort. In the two-dimensional space of interest it required the random selection of 2 numbers, RNR and RNS. The call, RAND (RN1), for the first random number, RN1, must be preceded by SAND (RN1). This sets up addresses in the congruence type of random-number generator subroutine of the Lewis computer library. This is a pseudo-random number generator inasmuch as each time SAND (RN1) is called the same sequence of random numbers is started again. Comparison of RNR and RNS with TWOP and TWOR determines in which directions the steps are taken. Step sizes and probabilities are held constant over MMAX(M, L) steps. After MMAX steps are taken the new location of the test particle is determined and tallied. Also after MMAX steps the energy transfer between the field and the test particle is determined and summed to that of the preceding N groups of MMAX steps.

If the test particle has not yet reached the loss cone, it is tallied according to the procedure on the lower right of the flow chart. It is simply located in one of the velocity space zones and credited to the corresponding element of a KTJK matrix. A certain probability exists for a particle to wander about indefinitely inside the mirror system without being lost. A walk length of 5000 MMAX steps was therefore set as a limit, after which the walk would be terminated and the next particle selected. The number of such walks was labeled IBAD.

When a test particle reaches a loss-cone boundary, the flow in the chart moves to the left. If it is the $AMAX^{th}$ particle, the tallying procedure in the lower left is followed. The marginal distributions in V and θ are then determined along with a counting of the total number of points (KTOT) tallied in the KTJK matrix. The sum of the values of N when the particles first reached a loss-cone boundary is printed out as SUM of NA.

Denote the collision frequency per test particle at X2 = $\pi/2$ and V2 = 1 by $\nu(\pi/2, 1)$; and define QUCOR by

$$\text{QUCOR} = \frac{\nu\left(\frac{\pi}{2}, 1\right) T_b^{3/2}}{n_b} \sqrt{\frac{m}{\text{Mass of a deuteron}}}$$

Then by use of equation (9g)

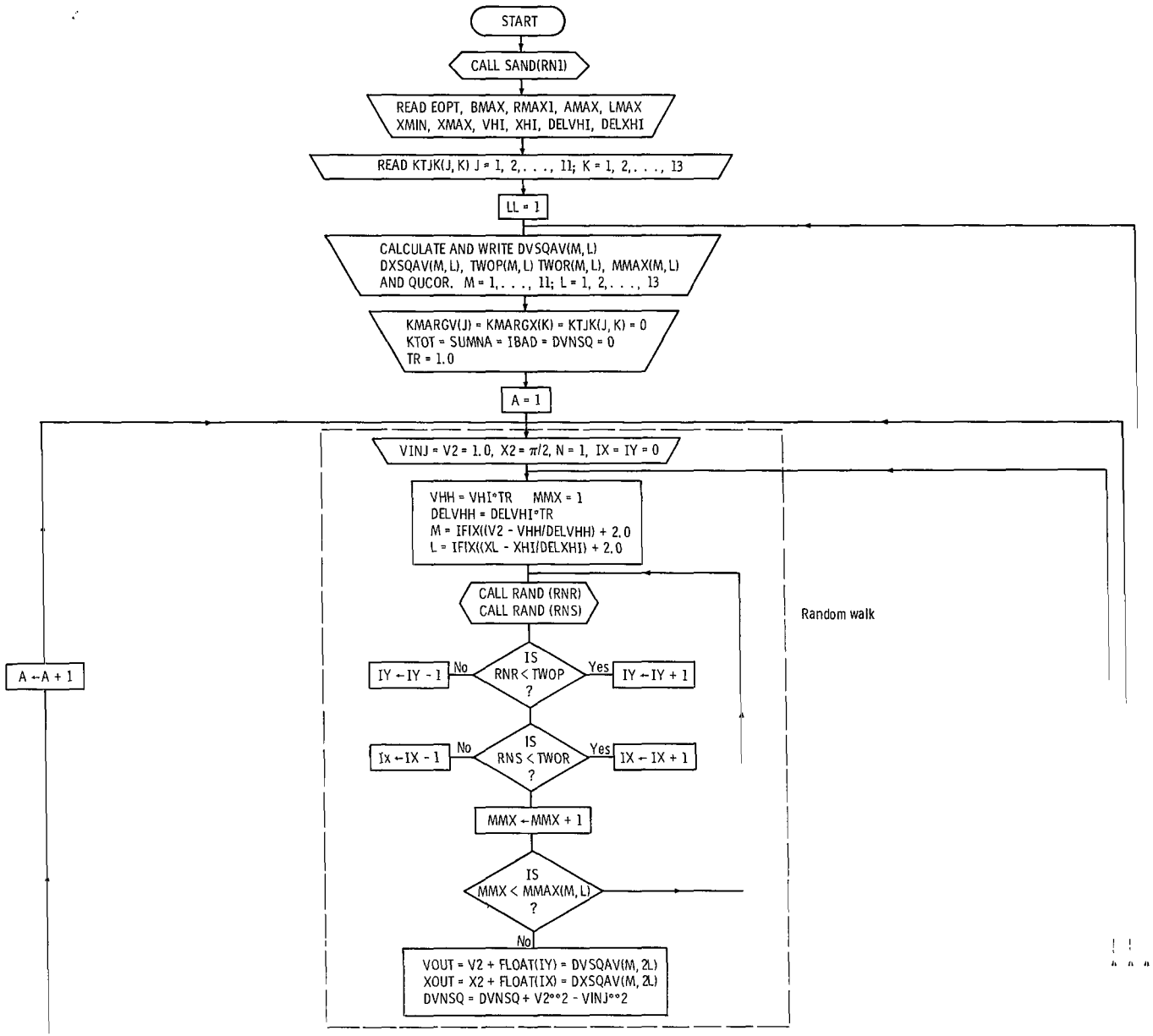
START
CALL SAND(RN1)
READ EOPT, BMAX, RMAX1, AMAX, LMAX
XMIN, XMAX, VHI, XHI, DELVHI, DELXHI
READ KTJK(J, K) J = 1, 2, . . ., 11; K = 1, 2, . . ., 13
LL = 1
CALCULATE AND WRITE DVSQAV(M, L)
DXSQAV(M, L), TWOP(M, L) TWOR(M, L), MMAX(M, L)
AND QUCOR. M = 1, . . ., 11; L = 1, 2, . . ., 13
KMARGV(J) = KMARGX(K) = KTJK(J, K) = 0
KTOT = SUMNA = IBAD = DVNSQ = 0
TR = 1.0
A = 1
VINJ = V2 = 1.0, X2 = π/2, N = 1, IX = IY = 0
VHH = VHI*TR MMX = 1
DELVHH = DELVHI*TR
M = IFIX((V2 - VHH/DELVHH) + 2.0
L = IFIX((XL - XHI/DELXHI) + 2.0
CALL RAND (RNR)
CALL RAND (RNS)
Random walk
IS RNR < TWOP ?
No
Yes
IY ← IY - 1
IY ← IY + 1
IS RNS < TWOR ?
No
Yes
IX ← IX - 1
IX ← IX + 1
MMX ← MMX + 1
IS MMX < MMAX(M, L) ?
No
VOUT = V2 + FLOAT(IY) = DVSQAV(M, 2L)
XOUT = X2 + FLOAT(IX) = DXSQAV(M, 2L)
DVNSQ = DVNSQ + V2**2 - VINJ**2
A ← A + 1

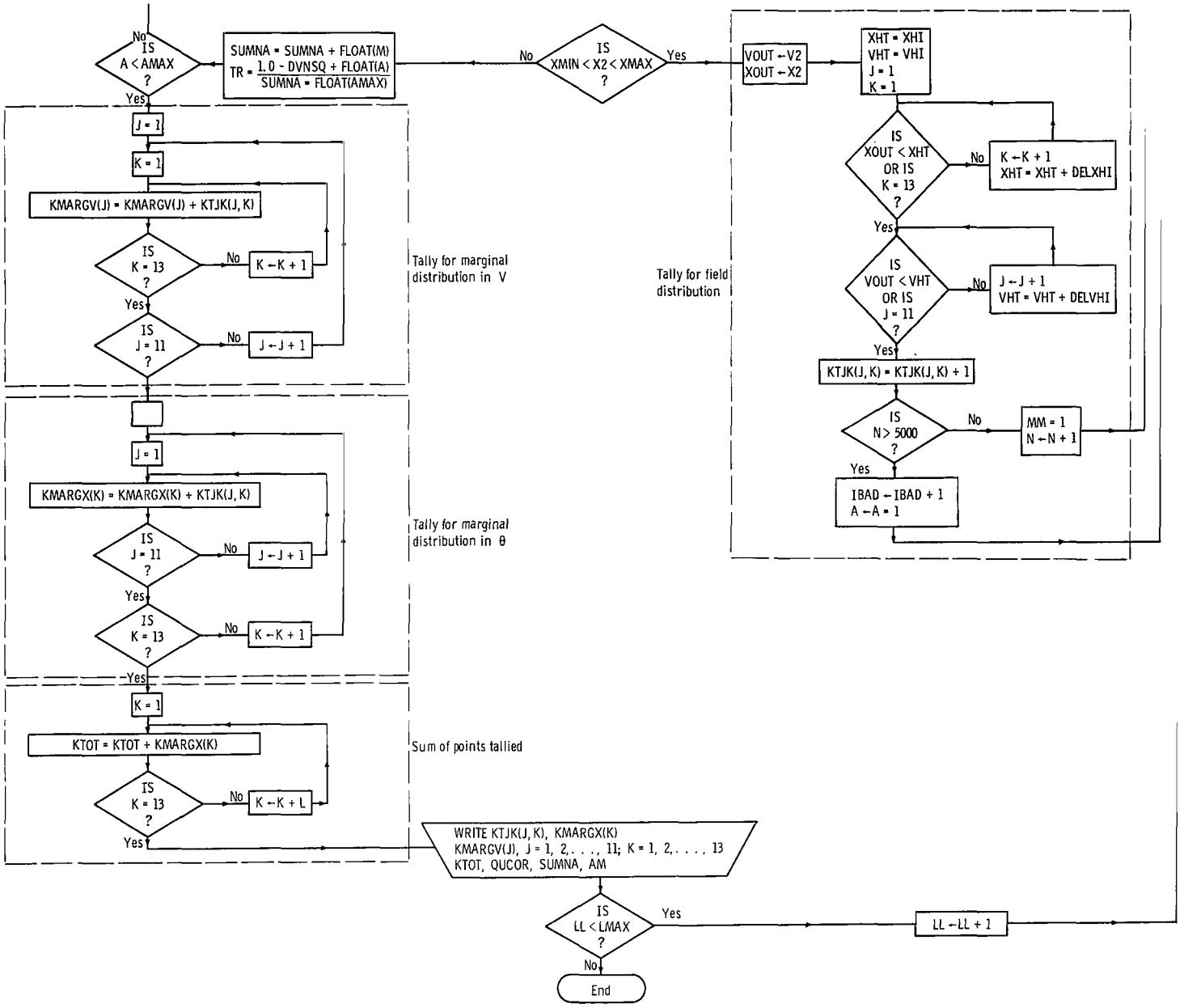

Figure 11. - Flow chart.

$$\text{QUCOR} = 0.896\times10^{-18}\,\beta^2\sqrt{\frac{E_o'}{T_b}}\sum_{J,K}\left[\frac{\text{KTJK(J, K)}}{\text{KTOT}}\sum_i w_i\sqrt{1+V_b^2-2V\cdot SK\cdot\cos x_i}\right]$$

for $z = 1$. The average number of Δ_τ time increments per walk is SUMNA divided by AMAX. The average number of walks per unit time multiplied by $\left(T_b^{3/2}/n_b\right)\sqrt{m/\text{Mass of a deuteron}}$ is then equal to (QUCOR · AMAX)/(SUMNA · RMAX1), and the loss rate parameter can be expressed as

$$\frac{\dot{n}T^{3/2}\sqrt{m}}{n^2} = \frac{0.578\times10^{-13}\,\text{QUCOR}\cdot\text{AMAX}}{\text{SUMNA}\cdot\text{RMAX1}}$$

After each walk, the field temperature is corrected to account for the energy transferred with the test particle. Assuming AMAX particles in the field ensemble results in

$$\frac{\Delta T_b}{T_b} = \frac{A}{\text{SUMNA}\cdot\text{AMAX}}\sum_{N=1}^{\text{SUMNA}}(V2^2 - \text{VINJ}^2) \qquad \text{(E2)}$$

The correction is applied through the dependence of step sizes and probabilities on $v\sqrt{m/2kT_b}$ as in equation (10).

After A reaches AMAX the resulting test-particle distributions are used to calculate new step size and probability matrices, and the iteration process in LL is continued until LL reaches LMAX.

FORTRAN SYMBOLS

A	test-particle number
AM	AMAX - IBAD
AMAX	size of test-particle sample
BMAX	impact parameter ratio
BRATIO	mirror ratio
CK	cos(X)
CRELi	$\cos\theta\cos\theta_b + \sin\theta\sin\theta_b\cos(\pi x_i)$

CX	cos(X2)
CXK	CX*CK
DELTAV(J, K)	$\overline{(\Delta V)}(J, K)$
DELTAX(J, K)	$\overline{\Delta\theta}(J, K)$
DELTHA	$\overline{(\Delta\theta)^2}$
DELVHH	DELVHI*TR
DELVHI	increment of V between successive J indices
DELVSQ	$\overline{(\Delta V)^2}$
DELXHI	increment of θ between successive K indices
DENOM1	$\sum_{J, K} KTJK(J, K)GND(J, K)$
DVNSQ	$\sum_{N=1}^{SUMNA} (V2^2 - VINJ^2)$
DVSQAV	$\sqrt{\overline{(\Delta V)^2}}$
DXSQAV	$\sqrt{\overline{(\Delta\theta)^2}}$
EOPT	E_o'/T_b
FDV	1.21/(SIB*EXP(Z*Z))
FDVi	Ti/Ui when i = 1, 2, 3, 4
FDVSi	$TT2^2/Ui$
FDXi	V*SRELi/Ui
FDXSi	1.0/FNUi - Y*SRELi**2/U2
FFVi	FNUi*FDVi*FDVSi
FMIXi	V*SRELi*FDVi
FNDi	SQRT(1.0+Y-2.0*V*SK*COS(πx_i))
FNUi	SQRT(W+Y-2.0*V2*V*(CRELi))
FPSIi	(Ti+V*CX*SRELi/Sx)/FNUi
FRICH(M, L)	2.25*S*NUM9/(W*NUM1)
FTERM(M, L)	-6.75*S*NUM6/NUM1

FTHEi	V*SRELi*(V2-2.0*CRELi-3.0*V2*Y(SRELi/FNUi)**2)/Ui
F(THETA)	KMARGX(K) *print out*
FV	ERF(Z) -R
F(V)	KMARGV(J) print out
GDV	$\sum_i w_i FDVi(x_i)$
GDVS	$\sum_i w_i FDVSi(x_i)$
GDX	$\sum_i w_i FDXi(x_i)$
GDXS	$\sum_i w_i FDXSi(x_i)$
GFV	$\sum_i w_i FFVi(x_i)$
GMIX	$\sum_i w_i FMIXi(x_i)$
GND	$\sum_i w_i FNDi(x_i)$
GNU	$\sum_i w_i FNUi(x_i)$
GPSI	$\sum_i w_i FPSIi(x_i)$
GTHE	$\sum_i w_i FTHEi(x_i)$
IBAD	number of walks discarded due to N reaching value 5000
IX	number of steps in positive θ direction
IY	number of steps in positive V direction

KJ(J)	number of points in J^{th} interval of injection distribution in V
KMARGV(J)	$\sum_{K}$KTJK(J, K) used for marginal distribution in V
KMARGX(K)	$\sum_{j}$ KTJK(J, K) used for marginal distribution in θ
KTJK(J, K)	tally of points in J^{th} increment of V and K^{th} increment of θ for field distribution determination
KTOT	$\sum_{j,k}$ KTJK(J, K)
LJ(J)	number of points in J^{th} increment of V in loss-cone distribution
LL	step number of iteration process
MMAX	number of steps between tally points
N	number of groups of MMAX steps
NA	number of groups of MMAX steps when particle reaches loss-cone boundary
NUM1, NUM2, . . ., NUM9	used in weighting functions by KTJK and summing over J and K
QUCOR	collision frequency at V2 = 1.0, X2 = $\pi/2$
R, RN1, RNR, RNS	random numbers selected from uniform distribution
RAND	call code for random numbers
RMAX	real MMAX
RMAX1	MMAX when V2 = 1.0 and X2 = $\pi/2$
S	$\frac{\ln \beta}{(E_o'\beta/T_b)^2}$
SAND	initial call code to set up addresses in random number generator
SIB	$\sqrt{T_b/E_o}$

SK	sin X
SRELi	$\sin\theta \cos\theta_b - \cos\theta \sin\theta_b \cos(\pi x_i)$
SUMNA	$\sum_{A=1}^{AMAX} NA$
SX	sin(X2)
SXK	sin(X2)sin(X)
Ti	V2-V*CRELi
TR	$1 - \Delta T_b/T_b$, see eq. (E2)
TTi	V*SQRT(1.0-CRELi**2)
TWOP	$2p_1$
TWOR	$2p_2$
Ui	FNUi**3
V	magnitude of field-particle velocity
V2	magnitude of test-particle velocity
VHH	VHI*TR
VHI	initial location on V scale for tallying particles
VHT	initial location on V scale for tallying particles
VINJ	injection velocity
VO	$\sqrt{1.5\ T_b/E'_o}\ \arcsin(R^2)$
VOUT	V2 value of point being tallied
VSQFV(J)	V^2 KMARG(J)
VSQFVT	$\sum_J V^2$ KMARGV(J)
VSQKJ(J)	V^2KJ(J)
VSQLJ(J)	V^2LJ(J)
VSQKJT	$\sum_J V^2$ KJ(J)
VSQLJT	$\sum_J V^2$ LJ(J)

W	$(V2)^2$
w_i	weight factors in Gaussian quadrature integration procedure
x_i	abscissa location in Gaussian quadrature integration procedure
X	θ_b
X2	θ
XHI	initial location on θ scale for tallying particles
XHT	initial location on θ scale for tallying particles
XMIN and XMAX	loss cone boundaries on θ
XOUT	X2 values of a point being tallied
Y	V^2
Z	$1.073\ VO\sqrt{E'_o/T_b}$
Subscripts:	
J	index on V or V2
K	index on X or X2
L	index on V2
M	index on X2
i	index on Gaussian quadrature terms

FORTRAN PROGRAM

```
      DIMENSION KMARGV(11),KMARGX(13),KTJK(11,13),KJ(11),LJ(11)
      DIMENSION DVSQAV(11,13),DXSQAV(11,13),TWOP(11,13),TWOR(11,13),
     1 MMAX(11,13),          VSQFV(11)
      DIMENSION DELTAV(11,13),DELTAX(11,13),DPSI(11,13),FTERM(11,13),
     1FRICH(11,13),DMIX(11,13)
      INTEGER A,AMAX
      CALL SAND(RN1)
C READ IN OF INITIAL FIELD DISTRIBUTION
      READ(5,502)((KTJK(J,K),J=1,11),K=1,13)
      READ(5,503)(KMARGV(J),J=1,11)
      READ(5,504)(KMARGX(K),K=1,13)
      READ(5,505)KTOT
  502 FORMAT(11I4)
  503 FORMAT(11I2)
  504 FORMAT(13I5)
  505 FORMAT(I5)
      WRITE(6,625)
      WRITE(6,628)(K,(KTJK(J,K),J=1,11),KMARGX(K),K=1,13)
      WRITE(6,629)(KMARGV(J),J=1,11)
      WRITE(6,630)KTOT
   10 READ(5,500)EOPT,BMAX,RMAX1,AMAX,LMAX
      IF(EOPT.EQ.0.)GO TO 170
      READ(5,501)XMIN,XMAX,VHI,XHI,DELVHI,DELXHI
      WRITE(6,600)EOPT,BMAX,RMAX1,AMAX,XMIN,XMAX
      BRATIO=1.0/(SIN(XMIN))**2
      WRITE(6,631)VHI,XHI,DELVHI,DELXHI,BRATIO
      DO 30 LL=1,LMAX
      TR=1.0
      S=ALOG(BMAX)/(EOPT*BMAX)**2
C ITERATION DO LOOP FOR SELF CONSISTENT FIELD DISTRIBUTION
      DO 29 L=1,13
C CALCULATION OF STEP SIZE AND PROBABILITY MATRICES
      DO 28 M=1,11
      V2=VHI+(FLOAT(M)-1.5)*DELVHI
      X2=XHI+(FLOAT(L)-1.5)*DELXHI
      A=V2**2
      CX=COS(X2)
      SX=SIN(X2)
      REAL NUM1,NUM2,NUM3,NUM4,NUM5,NUM6,NUM7,NUM8,NUM9
      NUM1=0.0
      NUM2=0.0
      NUM3=0.0
      NUM4=0.0
      NUM5=0.0
      NUM6=0.0
      NUM7=0.0
      NUM8=0.0
      NUM9=0.0
      DENOM1=0.0
C INTEGRATION OVER POLAR ANGLE AND VELOCITY BY QUADRATURES
      DO 31 K=1,13
```

```
      DO32J=1,11
      IF(LL-1)13,13,14
13    V=(0.200+(FLOAT(J)-1.5)*0.200)*SQRT(1.5/EOPT)
      X=0.241661+(FLOAT(K)-1.5)*0.241661
      GO TO 15
14    V=VHI+(FLOAT(J)-1.5)*DELVHI
      X=XHI+(FLOAT(K)-1.5)*DELXHI
15    Y=V**2
      CK=COS(X)
      SK=SIN(X)
      CXK=CX*CK
      SXK=SX*SK
C INTEGRATION OVER AZIMUTHAL ANGLE BY GAUSSIAN QUADRATURES
      CREL1=CXK+SXK*COS(0.18343*3.1416)
      SREL1=SX*CK-CX*SK*COS(0.18343*3.1416)
      FNU1=SQRT(W+Y-2.0*V2*V*CREL1)
      FND1=SQRT(1.0+Y-2.0*V*SK*COS(0.18343*3.1416))
      U1=FNU1**3
      T1=V2-V*CREL1
      TT1=V*SQRT(1.0-CREL1**2)
      FDX1=V*SREL1/U1
      FDV1=T1/U1
      FDVS1=TT1**2/U1
      FDXS1=1.0/FNU1-Y*SREL1**2/U1
      FFV1=FNU1*FDV1*FDVS1
      FPSI1=(T1+V*CX*SREL1/SX)/FNU1
      FMIX1=V*SREL1*FDV1
      FTHE1=V*SREL1*(V2-2.0*CREL1-3.0*V2*Y*(SREL1/FNU1)**2)/U1
      CREL2=CXK+SXK*COS(0.52553*3.1416)
      SREL2=SX*CK-CX*SK*COS(0.52553*3.1416)
      FNU2=SQRT(W+Y-2.0*V2*V*CREL2)
      FND2=SQRT(1.0+Y-2.0*V*SK*COS(0.52553*3.1416))
      U2=FNU2**3
      T2=V2-V*CREL2
      TT2=V*SQRT(1.0-CREL2**2)
      FDX2=V*SREL2/U2
      FDV2=T2/U2
      FDVS2=TT2**2/U2
      FDXS2=1.0/FNU2-Y*SREL2**2/U2
      FFV2=FNU2*FDV2*FDVS2
      FPSI2=(T2+V*CX*SREL2/SX)/FNU2
      FMIX2=V*SREL2*FDV2
      FTHE2=V*SREL2*(V2-2.0*CREL2-3.0*V2*Y*(SREL2/FNU2)**2)/U2
      CREL3=CXK+SXK*COS(0.79667*3.1416)
      SREL3=SX*CK-CX*SK*COS(0.79667*3.1416)
      FNU3=SQRT(W+Y-2.0*V2*V*CREL3)
      FND3=SQRT(1.0+Y-2.0*V*SK*COS(0.79667*3.1416))
      U3=FNU3**3
      T3=V2-V*CREL3
      TT3=V*SQRT(1.0-CREL3**2)
      FDX3=V*SREL3/U3
      FDV3=T3/U3
      FDVS3=TT3**2/U3
      FDXS3=1.0/FNU3-Y*SREL3**2/U3
      FFV3=FNU3*FDV3*FDVS3
      FPSI3=(T3+V*CX*SREL3/SX)/FNU3
```

```
      FMIX3=V*SREL3*FDV3
      FTHE3=V*SREL3*(V2-2.0*CREL3-3.0*V2*Y*(SREL3/FNU3)**2)/U3
      CREL4=CXK+SXK*COS(0.96029*3.1416)
      SREL4=SX*CK-CX*SK*COS(0.96029*3.1416)
      FNU4=SQRT(W+Y-2.0*V2*V*CREL4)
      FND4=SQRT(1.0+Y-2.0*V*SK*COS(0.96029*3.1416))
      L4=FNU4**3
      T4=V2-V*CREL4
      TT4=V*SQRT(1.0-CREL4**2)
      FDX4=V*SREL4/U4
      FDV4=T4/U4
      FDVS4=TT4**2/U4
      FDXS4=1.0/FNU4-Y*SREL4**2/U4
      FFV4=FNU4*FDV4*FDVS4
      FPSI4=(T4+V*CX*SREL4/SX)/FNU4
      FMIX4=V*SREL4*FDV4
      FTHE4=V*SREL4*(V2-2.0*CREL4-3.0*V2*Y*(SREL4/FNU4)**2)/U4
      GNU=0.36268*FNU1+0.31371*FNU2+0.22238*FNU3+0.10123*FNU4
      GND=0.36268*FND1+0.31371*FND2+0.22238*FND3+0.10123*FND4
      GDV=0.36268*FDV1+0.31371*FDV2+0.22238*FDV3+0.10123*FDV4
      GDX=0.36268*FDX1+0.31371*FDX2+0.22238*FDX3+0.10123*FDX4
      GDVS=0.36268*FDVS1+0.31371*FDVS2+0.22238*FDVS3+0.10123*FDVS4
      GDXS=0.36268*FDXS1+0.31371*FDXS2+0.22238*FDXS3+0.10123*FDXS4
      GFV=0.36268*FFV1+0.31371*FFV2+0.22238*FFV3+0.10123*FFV4
      GPSI=0.36268*FPSI1+0.31371*FPSI2+0.22238*FPSI3+0.10123*FPSI4
      GMIX=0.36268*FMIX1+0.31371*FMIX2+0.22238*FMIX3+0.10123*FMIX4
      GTHE=0.36268*FTHE1+0.31371*FTHE2+0.22238*FTHE3+0.10123*FTHE4
      NUM1=NUM1+FLOAT(KTJK(J,K))*GNU
      NUM2=NUM2+FLOAT(KTJK(J,K))*GDV
      NUM3=NUM3+FLOAT(KTJK(J,K))*GDX
      NUM4=NUM4+FLOAT(KTJK(J,K))*GDVS
      NUM5=NUM5+FLOAT(KTJK(J,K))*GDXS
      NUM6=NUM6+FLOAT(KTJK(J,K))*GFV
      NUM7=NUM7+FLOAT(KTJK(J,K))*GPSI
      NUM8=NUM8+FLOAT(KTJK(J,K))*GMIX
      NUM9=NUM9+FLOAT(KTJK(J,K))*GTHE
      DENOM1=DENOM1+FLOAT(KTJK(J,K))*GND
   32 CONTINUE
   31 CONTINUE
      RMAX=RMAX1*NUM1/DENOM1
      DELTAV(M,L)=-4.50*S*NUM2/NUM1
      DELTAX(M,L)=-4.50*S*NUM3/(V2*NUM1)
      DELVSQ=2.25*S*NUM4/NUM1
      DELTHA=2.25*S*NUM5/(W*NUM1)
      DVSQAV(M,L)=SQRT(DELVSQ)
      DXSQAV(M,L)=SQRT(DELTHA)
      FTERM(M,L)=-6.75*S*NUM6/NUM1
      DPSI(M,L)=2.25*S*NUM7/(W*V2*SX*SX*NUM1)
      DMIX(M,L)=2.25*S*NUM8/(V2*NUM1)
      FRICH(M,L)=2.25*S*NUM9/(W*NUM1)
      TWOP(M,L)=0.5*(1.0+(DELTAV(M,L)-FTERM(M,L)+0.5*V2*(DELTHA+SX**2*
     1DPSI(M,L)))/DVSQAV(M,L))
      TWOX(M,L)=0.5*(1.0+(DELTAX(M,L)-FRICH(M,L)-DMIX(M,L)/V2+0.5*SX*CX*
     1DPSI(M,L))/DXSQAV(M,L))
      NMAX(M,L)=IFIX(RMAX+0.5)
```

```
28      CONTINUE
29      CONTINUE
        CUCOR=0.896E-18*BMAX**2*SQRT(EOPT)* DENOM1 /FLOAT(KTOT)
        WRITE(6,624)LL
        WRITE(6,632)
        WRITE(6,633)(L,(DVSQAV(M,L),M=1,11),L=1,13)
        WRITE(6,634)
        WRITE(6,633)(L,(DXSQAV(M,L),M=1,11),L=1,13)
        WRITE(6,635)
        WRITE(6,633)(L,(TWOP(M,L),M=1,11),L=1,13)
        WRITE(6,636)
        WRITE(6,633)(L,(TWOR(M,L),M=1,11),L=1,13)
        WRITE(6,637)
        WRITE(6,638)(L,(MMAX(M,L),M=1,11),L=1,13)
        DO17J=1,11
        KMARGV(J)=0
        KJ(J)=0
        LJ(J)=0
        DO17K=1,13
        KMARGX(K)=0
17      KTJK(J,K)=0
        KTOT=0
        DVNSQ=0.0
        SUMNA=0.0
        IBAD=0
        SIB=1.0/SQRT(EOPT)
C START OF WALKING AMAX PARTICLES, ONE AT A TIME
        DO90A=1,AMAX
        CALL RAND(R)
C NEWTON RAPHSON DETERMINATION OF V(R) FROM R(V),  BUDKER'S  DISTRIBUTION
        VO=1.225*SIB*ARSIN(R*R)
1       Z=1.073*VO/SIB
        FV=ERF(Z)-R
        FDV=1.21/(SIB*EXP(Z*Z))
        F=FV/FDV
        V2=VO-F
        IF(ABS(F)-0.01)3,3,2
2       VO=V2
        GO TO 1
3       VINJ=V2
        VHT=0.1
C TALLY OF INJECTION MARGINAL DISTRIBUTION IN V
        DO4J=1,11
        IF(VINJ.LT.VHT)GO TO 5
4       VHT=VHT+0.15
        J=11
5       KJ(J)=KJ(J) +1
        X2=1.57079633
        A=1
21      VHH=VHI*TR
        DELVHH=DELVHI*TR
C LOCATION OF INDICES IN STEP SIZE AND PROBABILITY MATRICES
        M=IFIX((V2-VHH)/DELVHH+2.0)
        IF(M.LT.1)GO TO 18
        IF(M.GT.11)GO TO 20
        GO TO 19
```

```
 18     N=1
        GO TO 19
 20     N=11
 19     L=IFIX((X2-XHI)/DELXHI+2.0)
C RANDOM WALK PROPER
        IX=0
        IY=0
        MMX=MMAX(M,L)
        DO 25 MM=1,MMX
        CALL RANC(RNR)
        CALL RANC(RNS)
        IF(RNR.LE.TWOP(M,L))GO TO 22
        IY=IY-1
        GO TO 23
 22     IY=IY+1
 23     IF(RNS.LE.TWOR(M,L))GO TO 24
        IX=IX-1
        GO TO 25
 24     IX=IX+1
 25     CONTINUE
C LOCATING TEST PARTICLE IN VELOCITY SPACE
        V2=V2+FLOAT(IY)*DVSQAV(M,L)
        DVNSQ=DVNSQ+V2*V2-VINJ*VINJ
        X2=X2+FLOAT(IX)*DXSQAV(M,L)
        IF(X2.LT.XMIN.OR.X2.GT.XMAX)GO TO 86
        VOUT=V2
        XOUT=X2
        XHT=XHI
        VHT=VHI
C FIELD DISTRIBUTION TALLY
        DO 81 K=1,13
        IF(XOUT.LT.XHT)GO TO 82
 81     XHT=XHT+DELXHI
        K=13
 82     CONTINUE
        DO 83 J=1,11
        IF(VOUT.LT.VHT)GO TO 84
 83     VHT=VHT+DELVHI
        J=11
 84     KTJK(J,K)=KTJK(J,K)+1
        IF(N.GT.5000)GO TO 80
 85     N=N+1
        GO TO 21
 86     SUMNA=SUMNA+FLOAT(N)
C ACCOUNTING FOR FIELD ENERGY CHANGE
        TR1=1.0-DVNSQ*FLOAT(A)/(SUMNA*FLOAT(AMAX))
        IF(TR1-0.0)87,87,88
 87     TR=0.001
        GO TO 89
 88     TR=SQRT(TR1)
 89     CONTINUE
        VHT=VHI
C TALLY OF PARTICLES ENTERING LOSS CONE
        DO 7 J=1,11
        IF(V2.LT.VHT)GO TO 8
 7      VHT=VHT+DELVHI
```

```
      J=11
8     LJ(J)=LJ(J)+1
      GO TO 90
80    IBAD=IBAD+1
90    CONTINUE
91    AM=FLOAT(AMAX-IBAD)
      VSQFVT=0.0
C TALLY FOR MARGINAL DISTRIBUTION IN V AND THETA
      DO161J=1,11
      DO160K=1,13
160   KMARGV(J)=KMARGV(J)+KTJK(J,K)
      V=VHI+(FLOAT(J)-1.5)*DELVHI
C CALCULATION OF FIELD ENERGY
      VSQFV(J)=V*V*FLOAT(KMARGV(J))
      VSQFVT=VSQFVT+VSQFV(J)
161   CONTINUE
      DO163K=1,13
      DO162J=1,11
162   KMARGX(K)=KMARGX(K)+KTJK(J,K)
163   CONTINUE
      DO164K=1,13
164   KTOT=KTOT+KMARGX(K)
      WRITE(6,400)
      WRITE(6,401)(KJ(J),J=1,11)
      WRITE(6,625)
      WRITE(6,628)(K,(KTJK(J,K),J=1,11),KMARGX(K),K=1,13)
      WRITE(6,629)(KMARGV(J),J=1,11)
      WRITE(6,641)(VSQFV(J),J=1,11),VSQFVT
      WRITE(6,630)KTOT
      WRITE(6,530)QUCOR
      WRITE(6,402)
      WRITE(6,403)(LJ(J),J=1,11)
      WRITE(6,640)SUMNA,AM
      WRITE(6,600)EOPT,BMAX,RMAX1,AMAX,XMIN,XMAX
30    CONTINUE
      GO TO 10
170   STOP
400   FORMAT(1HL,45X,41HTALLY OF POINTS IN INJECTION DISTRIBUTION
     1/30X,3HJ=1,5X,3HJ=2,5X,3HJ=3,5X,3HJ=4,5X,3HJ=5,5X,3HJ=6,5X,3HJ=7,
     25X,3HJ=8,5X,3HJ=9,4X,4HJ=10,4X,4HJ=11)
401   FORMAT(10X,5HKJ(J),10X,11I8)
402   FORMAT(1HL,45X,41HTALLY OF POINTS IN LOSS CONE DISTRIBUTION
     1/30X,3HJ=1,5X,3HJ=2,5X,3HJ=3,5X,3HJ=4,5X,3HJ=5,5X,3HJ=6,5X,3HJ=7,
     25X,3HJ=8,5X,3HJ=9,4X,4HJ=10,4X,4HJ=11)
403   FORMAT(10X,5HLJ(J),10X,11I8)
500   FORMAT(F6.1,2(E14.7),I6,I3)
501   FORMAT(6(F10.8))
600   FORMAT(1H1,50X,23HRANDOM WALK CALCULATION/1H0,10X,7HEO'/T =,
     1 F6.1,5X,6HBMAX =,1PE10.3,5X,6HRMAX1=,1PE10.3,5X,5HAMAX=,I5,5X,
     2 5HXMIN=,0PF10.7,5X,5HXMAX=,F10.7)
624   FORMAT(1HL,55X,20HITERATION NUMBER LL=,I1)
625   FORMAT(1HL,42X,48HTOTAL TALLY OF NUMBER OF POINTS IN EACH INTERVAL
     1 /14X,1HK,15X,3HJ=1,5X,3HJ=2,5X,3HJ=3,5X,3HJ=4,5X,3HJ=5,5X,3HJ=6,
     2 5X,3HJ=7,5X,3HJ=8,5X,3HJ=9,4X,4HJ=10,4X,4HJ=11,3X,8HF(THETA))
628   FORMAT(10X,I5,10X,12I8)
629   FORMAT(11X,4HF(V),10X,11I8)
```

```
  630   FORMAT(1HL,5X,22HTOTAL POINTS TALLIED =,I10)
  530   FORMAT(6X,30HCOLLISION FREQUENCY PARAMETER=,E14.7)
  631   FORMAT(6X,4HVHI=,F10.7,5X,4HXHI=,F10.7,5X,7HDELVHI=,F10.7,5X,7HDEL
       1XHI=,F10.7,5X,13HMIRROR RATIO=,F11.7)
  632   FORMAT(1HL,55X,21HSTEP SIZE DXSQAV(M,L)
       1 /1X,2H L,7X,3HM=1,8X,3HM=2,8X,3HM=3,8X,3HM=4,8X,3HM=5,8X,3HM=6,
       2 8X,3HM=7,8X,3HM=8,8X,3HM=9,7X,4HM=10,7X,4HM=11)
  633   FORMAT(1X,I2,1X,11E11.3)
  634   FORMAT(1HL,55X,21HSTEP SIZE DXSQAV(M,L)
       1 /1X,2H L,7X,3HM=1,8X,3HM=2,8X,3HM=3,8X,3HM=4,8X,3HM=5,8X,3HM=6,
       2 8X,3HM=7,8X,3HM=8,8X,3HM=9,7X,4HM=10,7X,4HM=11)
  635   FORMAT(1HL,55X,21HPROBABILITY TWOP(M,L)
       1 /1X,2H L,7X,3HM=1,8X,3HM=2,8X,3HM=3,8X,3HM=4,8X,3HM=5,8X,3HM=6,
       2 8X,3HM=7,8X,3HM=8,8X,3HM=9,7X,4HM=10,7X,4HM=11)
  636   FORMAT(1HL,55X,21HPROBABILITY TWOR(M,L)
       1 /1X,2H L,7X,3HM=1,8X,3HM=2,8X,3HM=3,8X,3HM=4,8X,3HM=5,8X,3HM=6,
       2 8X,3HM=7,8X,3HM=8,8X,3HM=9,7X,4HM=10,7X,4HM=11)
  637   FORMAT(1HL,55X,21HFREQUENCY   MMAX(M,L)
       1 /1X,2H L,7X,3HM=1,8X,3HM=2,8X,3HM=3,8X,3HM=4,8X,3HM=5,8X,3HM=6,
       2 8X,3HM=7,8X,3HM=8,8X,3HM=9,7X,4HM=10,7X,4HM=11)
  638   FORMAT(1X,I2,1X,11I11)
  640   FORMAT(1HL,7HSUM NA=,1PE14.7,5X,3HAM=,1PE14.7)
  641   FORMAT(11X,6HVVE(V),8X,11F8.1,2X,F10.1)
        END
```

RANDOM WALK CALCULATION

EO'/T = 1.5 BMAX = 3.162E 02 RMAX1= 3.162E 01 AMAX= 500 XMIN= 1.1502463 XMAX= 1.9913463

VHI= 0.2000000 XHI= 1.2149463 DELVHI= 0.2000000 DELXHI= 0.0647000 MIRROR RATIO= 1.2000168

ITERATION NUMBER LL=1

STEP SIZE DVSQAV(M,L)

L	M=1	M=2	M=3	M=4	M=5	M=6	M=7	M=8	M=9	M=10	M=11
1	0.758E-02	0.721E-02	0.646E-02	0.553E-02	0.459E-02	0.374E-02	0.303E-02	0.245E-02	0.199E-02	0.164E-02	0.136E-02
2	0.758E-02	0.721E-02	0.646E-02	0.553E-02	0.458E-02	0.374E-02	0.302E-02	0.245E-02	0.199E-02	0.164E-02	0.136E-02
3	0.758E-02	0.721E-02	0.646E-02	0.552E-02	0.458E-02	0.373E-02	0.302E-02	0.245E-02	0.199E-02	0.164E-02	0.136E-02
4	0.758E-02	0.721E-02	0.646E-02	0.552E-02	0.458E-02	0.373E-02	0.302E-02	0.245E-02	0.199E-02	0.164E-02	0.136E-02
5	0.758E-02	0.722E-02	0.646E-02	0.552E-02	0.458E-02	0.373E-02	0.302E-02	0.245E-02	0.199E-02	0.164E-02	0.137E-02
6	0.758E-02	0.722E-02	0.646E-02	0.552E-02	0.458E-02	0.373E-02	0.302E-02	0.245E-02	0.199E-02	0.164E-02	0.137E-02
7	0.758E-02	0.722E-02	0.646E-02	0.552E-02	0.458E-02	0.373E-02	0.302E-02	0.245E-02	0.199E-02	0.164E-02	0.137E-02
8	0.758E-02	0.722E-02	0.646E-02	0.552E-02	0.458E-02	0.373E-02	0.302E-02	0.245E-02	0.199E-02	0.164E-02	0.137E-02
9	0.758E-02	0.722E-02	0.646E-02	0.552E-02	0.458E-02	0.373E-02	0.302E-02	0.245E-02	0.199E-02	0.164E-02	0.137E-02
10	0.758E-02	0.721E-02	0.646E-02	0.552E-02	0.458E-02	0.373E-02	0.302E-02	0.245E-02	0.199E-02	0.164E-02	0.136E-02
11	0.758E-02	0.721E-02	0.646E-02	0.552E-02	0.458E-02	0.373E-02	0.302E-02	0.245E-02	0.199E-02	0.164E-02	0.136E-02
12	0.758E-02	0.721E-02	0.646E-02	0.553E-02	0.458E-02	0.374E-02	0.302E-02	0.245E-02	0.199E-02	0.164E-02	0.136E-02
13	0.758E-02	0.721E-02	0.646E-02	0.553E-02	0.459E-02	0.374E-02	0.303E-02	0.245E-02	0.199E-02	0.164E-02	0.136E-02

STEP SIZE DXSQAV(M,L)

L	M=1	M=2	M=3	M=4	M=5	M=6	M=7	M=8	M=9	M=10	M=11
1	0.760E-01	0.245E-01	0.138E-01	0.914E-02	0.648E-02	0.481E-02	0.369E-02	0.290E-02	0.233E-02	0.191E-02	0.159E-02
2	0.760E-01	0.245E-01	0.138E-01	0.913E-02	0.648E-02	0.481E-02	0.368E-02	0.290E-02	0.233E-02	0.191E-02	0.159E-02
3	0.759E-01	0.245E-01	0.138E-01	0.912E-02	0.647E-02	0.480E-02	0.368E-02	0.290E-02	0.233E-02	0.191E-02	0.159E-02
4	0.759E-01	0.244E-01	0.138E-01	0.912E-02	0.647E-02	0.480E-02	0.368E-02	0.290E-02	0.233E-02	0.191E-02	0.159E-02
5	0.759E-01	0.244E-01	0.138E-01	0.912E-02	0.647E-02	0.480E-02	0.368E-02	0.290E-02	0.233E-02	0.191E-02	0.159E-02
6	0.759E-01	0.244E-01	0.138E-01	0.912E-02	0.647E-02	0.480E-02	0.368E-02	0.290E-02	0.233E-02	0.191E-02	0.159E-02
7	0.759E-01	0.244E-01	0.138E-01	0.911E-02	0.647E-02	0.480E-02	0.368E-02	0.290E-02	0.233E-02	0.191E-02	0.159E-02
8	0.759E-01	0.244E-01	0.138E-01	0.912E-02	0.647E-02	0.480E-02	0.368E-02	0.290E-02	0.233E-02	0.191E-02	0.159E-02
9	0.759E-01	0.244E-01	0.138E-01	0.912E-02	0.647E-02	0.480E-02	0.368E-02	0.290E-02	0.233E-02	0.191E-02	0.159E-02
10	0.759E-01	0.244E-01	0.138E-01	0.912E-02	0.647E-02	0.480E-02	0.368E-02	0.290E-02	0.233E-02	0.191E-02	0.159E-02
11	0.759E-01	0.245E-01	0.138E-01	0.912E-02	0.647E-02	0.480E-02	0.368E-02	0.290E-02	0.233E-02	0.191E-02	0.159E-02
12	0.760E-01	0.245E-01	0.138E-01	0.913E-02	0.648E-02	0.481E-02	0.368E-02	0.290E-02	0.233E-02	0.191E-02	0.159E-02
13	0.760E-01	0.245E-01	0.138E-01	0.914E-02	0.648E-02	0.481E-02	0.369E-02	0.290E-02	0.233E-02	0.191E-02	0.159E-02

PROBABILITY TWOP(M,L)

L	M=1	M=2	M=3	M=4	M=5	M=6	M=7	M=8	M=9	M=10	M=11
1	0.538E 00	0.511E 00	0.505E 00	0.503E 00	0.501E 00	0.500E 00	0.500E 00	0.499E 00	0.499E 00	0.499E 00	0.499E 00
2	0.538E 00	0.511E 00	0.505E 00	0.503E 00	0.501E 00	0.501E 00	0.500E 00	0.499E 00	0.499E 00	0.499E 00	0.499E 00
3	0.538E 00	0.511E 00	0.505E 00	0.503E 00	0.501E 00	0.501E 00	0.500E 00	0.499E 00	0.499E 00	0.499E 00	0.499E 00
4	0.537E 00	0.511E 00	0.505E 00	0.503E 00	0.501E 00	0.501E 00	0.500E 00	0.499E 00	0.499E 00	0.499E 00	0.499E 00
5	0.537E 00	0.511E 00	0.505E 00	0.503E 00	0.501E 00	0.501E 00	0.500E 00	0.499E 00	0.499E 00	0.499E 00	0.499E 00
6	0.537E 00	0.511E 00	0.505E 00	0.503E 00	0.501E 00	0.501E 00	0.500E 00	0.499E 00	0.499E 00	0.499E 00	0.499E 00
7	0.537E 00	0.511E 00	0.505E 00	0.503E 00	0.501E 00	0.501E 00	0.500E 00	0.499E 00	0.499E 00	0.499E 00	0.499E 00
8	0.537E 00	0.511E 00	0.505E 00	0.503E 00	0.501E 00	0.501E 00	0.500E 00	0.499E 00	0.499E 00	0.499E 00	0.499E 00
9	0.537E 00	0.511E 00	0.505E 00	0.503E 00	0.501E 00	0.501E 00	0.500E 00	0.499E 00	0.499E 00	0.499E 00	0.499E 00
10	0.537E 00	0.511E 00	0.505E 00	0.503E 00	0.501E 00	0.501E 00	0.500E 00	0.499E 00	0.499E 00	0.499E 00	0.499E 00
11	0.538E 00	0.511E 00	0.505E 00	0.503E 00	0.501E 00	0.501E 00	0.500E 00	0.499E 00	0.499E 00	0.499E 00	0.499E 00
12	0.538E 00	0.511E 00	0.505E 00	0.503E 00	0.501E 00	0.501E 00	0.500E 00	0.499E 00	0.499E 00	0.499E 00	0.499E 00
13	0.538E 00	0.511E 00	0.505E 00	0.503E 00	0.501E 00	0.500E 00	0.500E 00	0.499E 00	0.499E 00	0.499E 00	0.499E 00

PROBABILITY TWOR(M,L)

L	M=1	M=2	M=3	M=4	M=5	M=6	M=7	M=8	M=9	M=10	M=11
1	0.511E 00	0.504E 00	0.502E 00	0.501E 00	0.501E 00	0.501E 00	0.500E 00	0.500E 00	0.500E 00	0.500E 00	0.500E 00
2	0.509E 00	0.503E 00	0.502E 00	0.501E 00	0.501E 00	0.500E 00	0.500E 00	0.500E 00	0.500E 00	0.500E 00	0.500E 00
3	0.507E 00	0.503E 00	0.501E 00	0.501E 00	0.501E 00	0.500E 00	0.500E 00	0.500E 00	0.500E 00	0.500E 00	0.500E 00
4	0.506E 00	0.502E 00	0.501E 00	0.501E 00	0.500E 00	0.500E 00	0.500E 00	0.500E 00	0.500E 00	0.500E 00	0.500E 00
5	0.504E 00	0.501E 00	0.501E 00	0.500E 00	0.500E 00	0.500E 00	0.500E 00	0.500E 00	0.500E 00	0.500E 00	0.500E 00
6	0.502E 00	0.501E 00	0.500E 00	0.500E 00	0.500E 00	0.500E 00	0.500E 00	0.500E 00	0.500E 00	0.500E 00	0.500E 00
7	0.500E 00	0.500E 00	0.500E 00	0.500E 00	0.500E 00	0.500E 00	0.500E 00	0.500E 00	0.500E 00	0.500E 00	0.500E 00
8	0.498E 00	0.499E 00	0.500E 00	0.500E 00	0.500E 00	0.500E 00	0.500E 00	0.500E 00	0.500E 00	0.500E 00	0.500E 00
9	0.496E 00	0.499E 00	0.499E 00	0.500E 00	0.500E 00	0.500E 00	0.500E 00	0.500E 00	0.500E 00	0.500E 00	0.500E 00
10	0.495E 00	0.498E 00	0.499E 00	0.499E 00	0.500E 00	0.500E 00	0.500E 00	0.500E 00	0.500E 00	0.500E 00	0.500E 00
11	0.493E 00	0.497E 00	0.499E 00	0.499E 00	0.499E 00	0.500E 00	0.500E 00	0.500E 00	0.500E 00	0.500E 00	0.500E 00
12	0.491E 00	0.497E 00	0.498E 00	0.499E 00	0.499E 00	0.500E 00	0.500E 00	0.500E 00	0.500E 00	0.500E 00	0.500E 00
13	0.489E 00	0.496E 00	0.498E 00	0.499E 00	0.499E 00	0.499E 00	0.500E 00	0.500E 00	0.500E 00	0.500E 00	0.500E 00

FREQUENCY MMAX(M,L)

L	M=1	M=2	M=3	M=4	M=5	M=6	M=7	M=8	M=9	M=10	M=11
1	22	23	25	27	30	33	37	41	45	49	54
2	22	23	25	27	30	33	37	41	45	50	54
3	22	23	25	27	30	33	37	41	45	50	54
4	22	23	25	27	30	33	37	41	45	50	54
5	22	23	25	27	30	33	37	41	45	50	54
6	22	23	25	27	30	33	37	41	45	50	54
7	22	23	25	27	30	33	37	41	45	50	54
8	22	23	25	27	30	33	37	41	45	50	54
9	22	23	25	27	30	33	37	41	45	50	54
10	22	23	25	27	30	33	37	41	45	50	54
11	22	23	25	27	30	33	37	41	45	50	54
12	22	23	25	27	30	33	37	41	45	50	54
13	22	23	25	27	30	33	37	41	45	49	54

TALLY OF POINTS IN INJECTION DISTRIBUTION

	J=1	J=2	J=3	J=4	J=5	J=6	J=7	J=8	J=9	J=10	J=11
KJ(J)	72	92	93	65	60	46	30	19	15	2	6

TOTAL TALLY OF NUMBER OF POINTS IN EACH INTERVAL

K	J=1	J=2	J=3	J=4	J=5	J=6	J=7	J=8	J=9	J=10	J=11	F(THETA)
1	17	61	143	184	224	191	265	118	7	0	37	1247
2	54	111	288	423	525	561	702	274	53	4	109	3104
3	25	200	434	745	889	989	782	428	76	104	255	4927
4	28	251	496	1055	1125	1504	772	431	121	272	404	6459
5	88	269	650	1204	1215	1900	1462	486	182	323	589	8368
6	42	297	828	1419	1561	2337	1706	807	280	369	409	10055
7	127	365	1041	1447	1960	2352	1859	1249	493	650	230	11773
8	46	326	837	1523	1857	1759	1380	1109	568	493	141	10039
9	91	324	635	1234	1505	1532	1044	704	639	328	162	8198
10	33	224	492	911	1187	1416	686	529	597	232	135	6442
11	21	168	313	667	866	1224	610	427	299	299	59	4993
12	59	115	247	388	595	850	482	246	163	200	36	3401
13	12	68	133	177	252	387	275	104	99	112	65	1684
F(V)	643	2779	6537	11377	13761	17002	12025	6912	3597	3386	2671	
VVF(V)	6.4	250.1	1634.2	5574.7	11146.4	20572.4	20322.2	15552.0	10395.3	12223.5	11779.1	109456.5

TOTAL POINTS TALLIED = 80690

COLLISION FREQUENCY PARAMETER= 0.1454641E-12

TALLY OF POINTS IN LOSS CONE DISTRIBUTION

	J=1	J=2	J=3	J=4	J=5	J=6	J=7	J=8	J=9	J=10	J=11
LJ(J)	128	121	77	69	43	33	13	9	4	1	1

SUM NA= 7.6188000E 04 AM= 4.9899999E 02

APPENDIX F

ANALYTICAL SOLUTION FOR CASE OF SHORT WALKS

Consider the walks so short that the Fokker-Planck coefficients are constant over the distance traveled. Assume that the walk terminates when a particle first reaches a prescribed θ distance from its initial location. Effects of V are thus of second order and can be neglected. For a spherical field distribution, both equations (4) and (5) in combination with a source term as in equation (6) reduce to

$$\frac{1}{2}\langle(\Delta\theta)^2\rangle \frac{\partial}{\partial\theta}\left(\sin\theta \frac{\partial f}{\partial\theta}\right) = -\dot{s}\sin\theta \tag{F1}$$

If the initial test-particle location is at $\theta \approx \pi/2$, then $\sin\theta \approx 1$ and $\dot{s} = \dot{s}_o\delta[\theta - (\pi/2)]$ reducing equation (F1) to

$$\frac{1}{2}\langle(\Delta\theta)^2\rangle \frac{\partial^2 f}{\partial\theta^2} = -s_o\delta\left(\theta - \frac{\pi}{2}\right) \tag{F2}$$

This model may simulate the end loss problem for mirror ratios very close to 1.0. Injection would be normal to the B field at a constant rate $\dot{s}_o$. The boundary conditions are

$$f(\theta_c) = f(\pi - \theta_c) = 0 \tag{F3}$$

Using (F1) in (F2) and integrating both sides of the equation gives

$$\frac{\partial f}{\partial\theta} - \frac{\partial f}{\partial\theta}\bigg|_{\theta=\theta_c} = -\frac{2\dot{s}_o}{\langle(\Delta\theta)^2\rangle} H\left(\theta - \frac{\pi}{2}\right)$$

where H is the Heaviside unit function. Integrating a second time and using equation (F3) yields

$$\left.\begin{aligned} f(\theta) - \left.\frac{\partial f}{\partial \theta}\right|_{\theta=\theta_c} (\theta - \theta_c) &= 0 && \text{when } \theta_c \le \theta \le \frac{\pi}{2} \\ &= -\frac{2\dot{s}_o}{\langle(\Delta\theta)^2\rangle}\left(\theta - \frac{\pi}{2}\right) && \text{when } \frac{\pi}{2} \le \theta \le (\pi - \theta_c) \end{aligned}\right\} \quad \text{(F4)}$$

At $\theta = \pi - \theta_c$

$$\left.\frac{\partial f}{\partial \theta}\right|_{\theta=\theta_c} = \frac{\dot{s}_o}{\langle(\Delta\theta)^2\rangle} \quad \text{(F5)}$$

Using equation (F5) in (F4) gives

$$\left.\begin{aligned} f(\theta) &= \frac{\dot{s}_o}{\langle(\Delta\theta)^2\rangle}(\theta - \theta_c) && \text{when } \theta_c \le \theta \le \frac{\pi}{2} \\ &= \frac{\dot{s}_o}{\langle(\Delta\theta)^2\rangle}(\pi - \theta - \theta_c) && \text{when } \frac{\pi}{2} \le \theta \le \pi \le \theta_c \end{aligned}\right\} \quad \text{(F6)}$$

Loss rate must equal injection rate for steady state so

$$\dot{n} = \int_{\theta_c}^{\pi-\theta_c} \dot{s}(\theta)\sin\theta\, d\theta = \dot{s}_o \int_{\theta_c}^{\pi-\theta_c} \delta\left(\theta - \frac{\pi}{2}\right)\sin\theta\, d\theta = \dot{s}_o$$

The number density, distribution function relation must be

$$n_b = \int_{\theta_c}^{\pi-\theta_c} f(\theta)\sin\theta\, d\theta = \frac{2\dot{s}_o}{\langle(\Delta\theta)^2\rangle} \int_{\theta_c}^{\pi/2} (\theta - \theta_c)\sin\theta\, d\theta$$

$$= \frac{2\dot{s}_o}{\langle(\Delta\theta)^2\rangle}(1 - \sin\theta_c) \quad \text{(F7)}$$

Using equation (F6) gives

$$\dot{n} = \frac{n_b \langle (\Delta\theta)^2 \rangle}{2(1 - \sin \theta_c)}$$

For small $\frac{\pi}{2} - \theta_c$,

$$\sin \theta_c = 1 - \frac{\left(\frac{\pi}{2} - \theta_c\right)^2}{2} \tag{F8}$$

to second order so that the loss rate becomes

$$\dot{n} = \frac{n_b \langle (\Delta\theta)^2 \rangle}{\left(\frac{\pi}{2} - \theta_c\right)^2} \tag{F9}$$

Evaluating $\langle (\Delta\theta)^2 \rangle$ for a spherical Maxwellian field distribution (eq. (11c)) and substituting into equation (F9) yields for $v = v_o$

$$\dot{n}\left(\frac{\pi}{2} - \theta_c\right)^2 = \frac{n_b^2}{\sqrt{m}} \frac{(Z_e)^4}{4\pi E_o'} \left(\frac{T_b}{E_o'}\right)^2 \frac{\ln \beta}{(2kT_b)^{3/2}} \left[\frac{1}{\sqrt{\pi}} e^{-E_o'/T_b} + \left(\sqrt{\frac{E_o'}{T_b}} - \frac{1}{2\sqrt{\frac{E_o'}{T_b}}} \right) \operatorname{erf} \sqrt{\frac{E_o'}{T_b}} \right] \tag{F10}$$

If the particles are, for example, injected at 10 times the average field energy then

$$\frac{1}{2} m v_o^2 = \frac{30}{2} kT_b$$

or

$$\frac{E_o'}{T_b} = 15$$

and for deuterons, for example,

$$\frac{nT_b^{3/2}\left(\frac{\pi}{2} - \theta_c\right)^2}{n_b^2 \log \beta} = 0.773\times10^{-19} \tag{F11}$$

This result is used in figure 6.

It is interesting to compare equation (F9) with equation (33) of reference 8. The result of reference 8, derived strictly from a random walk, is for only one absorbing wall. The loss rate predicted by equation (F9) (for two absorbing walls) is just twice that of reference 7.

To determine the marginal distribution in θ for use on figure 7(a) substitute equations (F7) and (F8) into (F6). This yields

$$\left.\begin{aligned} F_\theta(\theta) = \frac{f_\theta(\theta)}{n_b} &= \frac{\theta - \theta_c}{\left(\frac{\pi}{2} - \theta_c\right)^2} && \text{when } \theta_c \le \theta \le \frac{\pi}{2} \\ &= \frac{1}{\frac{\pi}{2} - \theta_c}\left(1 + \frac{\frac{\pi}{2} - \theta}{\frac{\pi}{2} - \theta_c}\right) && \text{when } \frac{\pi}{2} \le \theta \le (\pi - \theta_c) \end{aligned}\right\} \tag{17}$$

APPENDIX G

SELECTION OF RANDOM NUMBERS FROM THE NONUNIFORM INJECTION DISTRIBUTION OF REFERENCE 5

The simulation procedure of sampling from a nonuniform distribution when the computer library contains only a uniformly distributed set of random numbers is quite common (refs. 9, 21, and pp. 252-264 of ref. 15). The relation between a uniformly distributed random number R and an arbitrarily distributed random number v is

$$R = \int_0^R dr = \int_0^{\mathscr{V}} f(v)dv$$

where it is necessary only that the second integral be a monotone increasing function of $\mathscr{V}$. This says that the cumulative distribution function R of the probability density f(v) is uniformly distributed in $\mathscr{V}$. If f(v) is integrable, $R(\mathscr{V})$ can be found. But to find $\mathscr{V}(R)$ explicitly in the case of interest herein required a root finding method such as, for example, the Newton-Raphson method (ref. 22).

The injection distribution of reference 5 is

$$R(\mathscr{V}) = \frac{\displaystyle\int_0^{\mathscr{V}} \langle(\Delta\theta)^2\rangle e^{-mv^2/2kT_b} v^2 \, dv}{\displaystyle\int_0^{\infty} \langle(\Delta\theta)^2\rangle e^{-mv^2/2kT_b} v^2 \, dv}$$

where $\langle(\Delta\theta)^2\rangle$ is given by equation (11c). Letting $x = \sqrt{m/2kT_b}\, v$ results in a new expression for $R(\mathscr{V})$:

$$R(\mathscr{V}) = \frac{\displaystyle\int_0^{\sqrt{m/2kT_b}\,\mathscr{V}} \frac{1}{x^2}\left[\frac{1}{\sqrt{\pi}}e^{-x^2} + \left(x - \frac{1}{2x}\right)\operatorname{erf} x\right]e^{-x^2}\,dx}{\displaystyle\int_0^{\infty} \frac{1}{x^2}\left[\frac{1}{\sqrt{\pi}}e^{-x^2} + \left(x - \frac{1}{2x}\right)\operatorname{erf} x\right]e^{-x^2}\,dx} \qquad \text{(G1)}$$

This was integrated by the method of Gaussian quadratures. The curve fit

$$R(\mathscr{V}) = \operatorname{erf}\left(1.073\sqrt{\frac{m}{2kT_b}}\,\mathscr{V}\right)$$

is a good approximation to the result. This is shown on figure 12 where $V = \mathscr{V}/v_o$ is

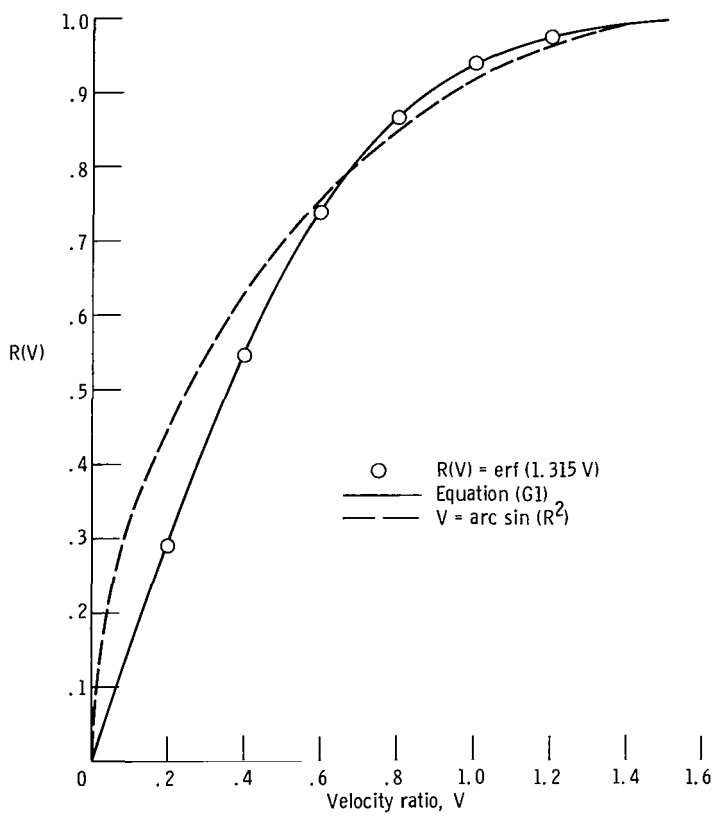

Figure 12. - Random number distribution to fit injection distribution of reference 5.

used as the abscissa and $\sqrt{m/2kT_b}\ v_o = \sqrt{E'_o/T_b}$ was set equal to $\sqrt{3/2}$ to make reference velocity v_o equal to the mean field velocity.

For an initial approximation V(R) for use in the Newton-Raphson method, the curve

$$V = \arcsin R^2$$

was used.

Results of this procedure to generate the injection distribution is shown to be satisfactory in figure 8(c).

REFERENCES

1. Kittel, Charles: Elementary Statistical Physics. John Wiley & Sons, Inc., 1958.
2. Feller, William: An Introduction to Probability Theory and Its Applications. Vol. I. Second ed., John Wiley & Sons, Inc., 1959.
3. Judd, David; MacDonald, William; and Rosenbluth, Marshall: End Leakage Losses from the Mirror Machine. Rep. UCRL-2931, Univ. California Radiation Lab., Mar. 25, 1955.
4. Wu, Ta-You: Kinetic Equations of Gases and Plasmas. Addison-Wesley Publ. Co., 1966.
5. Sivukhin, D. V.: Coulonb Collisions in a Fully Ionized Plasma. Vol. 4 of Reviews of Plamsa Physics. M. A. Leontovich, ed., Consultants Bureau, 1966, pp. 93-241.
6. Allis, W. P.: Motion of Ions and Electrons. Tech. Rep. 299, Massachusetts Inst. Tech. Res. Lab. Electronics, June 13, 1956.
7. Chandrasekhar, S.: Dynamical Friction. I. General Considerations: The Coefficient of Dynamical Friction. Astrophys. J., vol. 97, Mar. 1943, pp. 255-273.
8. Chandrasekhar, S.: Stochastic Problems in Physics and Astronomy. Rev. Mod. Phys., vol. 15, no. 1, Jan. 1943, pp. 1-89.
9. Perlmutter, Morris: Monte Carlo Solution for the Characteristics of a Highly Rarefied Ionized Gas Flowing Through a Channel with a Transverse Magnetic Field. NASA TN D-2211, 1964.
10. Goldstein, Charles M.: Monte Carlo Method for the Calculation of Transport Properties in a Low-Density Ionized Gas. NASA TN D-2959, 1965.
11. Rosenbluth, Marshall N.; MacDonald, William M.; and Judd, David L.: Fokker-Planck Equation for an Inverse-Square Force. Phys. Rev., vol. 107, no. 1, July 1, 1957, pp. 1-6.
12. Spitzer, Lyman: Physics of Fully Ionized Gases. Interscience Publ. Inc., New York, 1956.
13. Roberts, John E.; and Carr, Marlene L.: End-Losses from Mirror Machines. Rep. UCRL-5651-T, Univ. California Lawrence Radiation Lab., Apr. 1960.
14. Post, R. F.; and Rosenbluth, M. N.: Electrostatic Instabilities in Finite Mirror-Confined Plasmas. Phys. Fluids, vol. 9, no. 4, Apr. 1966, pp. 730-749.
15. Shreider, Yu. A., ed.: Method of Statistical Testing, Monte Carlo Method. Elsevier Publ. Co., 1964.

16. Linhart, J. G.: Plasma Physics. Interscience Publ. Inc., 1960.

17. Ben Daniel, David J.: A Theory of Scattering Loss from a Magnetic Mirror System. Rep. UCRL-6236, Univ. California Laurence Radiation Lab., Mar. 7, 1961.

18. Chapman, Sydney; and Cowling, T. G.: The Mathematical Theory of Nonuniform Gases. Second ed., Cambridge University Press, 1952.

19. Budker, G. I.: Thermonuclear Reactions in a System with Magnetic Stoppers, and the Problem of Direct Transportation of Thermonuclear Energy into Electrical Energy. Vol. 3 of Plasma Physics and the Problem of Controlled Thermonuclear Reactions. M. A. Leontovich, ed., Pergamon Press, 1959, pp. 1-33.

20. Kaufman, Allan N.: Ambipolar Effects in Mirror Losses. Conference on Controlled Thermonuclear Reactions. AEC Rep. TID-7520, Pt. 2, Sept. 1956, p. 387.

21. Meyer, Herbert A., ed.: Symposium on Monte Carlo Methods. John Wiley & Sons, Inc., 1956.

22. Golden, James T.: Fortran IV: Programming and Computing. Prentice-Hall, Inc., 1965.

NASA-Langley, 1970 —— 25 E-5165

"The aeronautical and space activities of the United States shall be conducted so as to contribute . . . to the expansion of human knowledge of phenomena in the atmosphere and space. The Administration shall provide for the widest practicable and appropriate dissemination of information concerning its activities and the results thereof."

—NATIONAL AERONAUTICS AND SPACE ACT OF 1958

NASA SCIENTIFIC AND TECHNICAL PUBLICATIONS

TECHNICAL REPORTS: Scientific and technical information considered important, complete, and a lasting contribution to existing knowledge.

TECHNICAL NOTES: Information less broad in scope but nevertheless of importance as a contribution to existing knowledge.

TECHNICAL MEMORANDUMS: Information receiving limited distribution because of preliminary data, security classification, or other reasons.

CONTRACTOR REPORTS: Scientific and technical information generated under a NASA contract or grant and considered an important contribution to existing knowledge.

TECHNICAL TRANSLATIONS: Information published in a foreign language considered to merit NASA distribution in English.

SPECIAL PUBLICATIONS: Information derived from or of value to NASA activities. Publications include conference proceedings, monographs, data compilations, handbooks, sourcebooks, and special bibliographies.

TECHNOLOGY UTILIZATION PUBLICATIONS: Information on technology used by NASA that may be of particular interest in commercial and other non-aerospace applications. Publications include Tech Briefs, Technology Utilization Reports and Notes, and Technology Surveys.

Details on the availability of these publications may be obtained from:

SCIENTIFIC AND TECHNICAL INFORMATION DIVISION

NATIONAL AERONAUTICS AND SPACE ADMINISTRATION

Washington, D.C. 20546